Regulatory Peptides 151 (2008) 164–169

Contents lists available at ScienceDirect

Regulatory Peptides

journal homepage: www.elsevier.com/locate/regpep

Triiodothyronine (T3) stimulates food intake via enhanced hypothalamic AMP-activated kinase activity

Shinya Ishii [a,*], Jun Kamegai [a,b], Hideki Tamura [a], Takako Shimizu [a], Hitoshi Sugihara [a], Shinichi Oikawa [a]

[a] Department of Medicine, Nippon Medical School, 1-1-5 Sendagi, Bunkyo-ku, Tokyo 113-8603, Japan
[b] Umigame Medical Clinic (J.K.), 2-17-16 Higashi-Kanamachi, Katsushika-ku, Tokyo 125-0041, Japan

ARTICLE INFO

Article history:
Received 29 March 2008
Received in revised form 22 July 2008
Accepted 24 July 2008
Available online 29 July 2008

Keywords:
Food intake
Hypothalamus
Leptin
Neuropeptides
Thyroid hormone

ABSTRACT

Thyroid hormone regulates food intake. We previously reported that rats with triiodothyronine (T3)-induced thyrotoxicosis display hyperphagia associated with suppressed circulating leptin levels, increased hypothalamic neuropeptide Y (NPY) mRNA and decreased hypothalamic pro-opiomelanocortin (POMC) mRNA. AMP-activated kinase (AMPK) is a serine/threonine protein kinase that is activated when cellular energy is depleted. We hypothesized that T3 causes an increase in hypothalamic AMPK activity, which in turn contributes to the development of T3-induced hyperphagia. Rats that were given s.c. injections of T3 (4.5 nmol/kg) had increased food intake 2 h later without alterations in NPY and POMC mRNA levels, but with increased hypothalamic phosphorylated AMPK (169%) and phosphorylated acetyl-CoA carboxylase (194%). To determine the more chronic effects of T3, rats were given 6 daily s.c. injection of T3 or the vehicle. Food intake was significantly increased. Multiple T3 injections increased hypothalamic phosphorylated AMPK (278%) and phosphorylated acetyl-CoA carboxylase (335%) compared to the controls. Intracerebroventricular administration of compound C, an AMPK inhibitor, blocked the food intake induced by a single or multiple injections of T3. Taken together, these results suggest that enhanced hypothalamic AMPK phosphorylation contributes to T3-induced hyperphagia. Hypothalamic AMPK plays an important role in the regulation of food intake and body weight.

1. Introduction

Thyroid hormone stimulates many metabolic processes, including energy expenditure and the metabolism of lipids, carbohydrates, proteins, and minerals. These stimulatory actions, especially the increase in energy expenditure, contribute to the clinical manifestations of thyrotoxicosis. Therefore, thyrotoxicosis causes weight loss and promotes increases in food intake in both humans and rodents [1,2]. We previously reported that rats with triiodothyronine (T3)-induced thyrotoxicosis display hyperphagia associated with suppressed circulating leptin levels, increased hypothalamic neuropeptide Y (NPY) mRNA levels and decreased hypothalamic pro-opiomelanocortin (POMC) mRNA levels. The decrease in plasma leptin observed in T3-induced thyrotoxicosis suggests that leptin is the most important peripheral signal regulating food intake [3]. Recently, Kong et al. [4] demonstrated that both acute and chronic administration of the low-dose of T3 that we used could stimulate food intake without altering plasma leptin levels. These results suggested that T3 directly affects food intake. However, the mechanism for the direct regulation of food intake by T3 is not clear.

Some lines of evidence indicate that AMP-activated protein kinase (AMPK) regulates food intake [5–7]. AMPK is a major regulator of energy utilization. It has been reported that AMPK is activated by metabolic stresses that deplete cellular ATP [8,9]. When ATP levels are depleted, there is a corresponding increase in intracellular AMP levels and AMPK is activated by phosphorylation of the catalytic subunit (α) by at least one upstream AMPK kinase (AMPKK). AMPK is expressed in the hypothalamic neurons involved in the regulation of food intake [5], where it may act to restore the depleted energy. Therefore, hypothalamic AMPK has an important role in the central regulation of food intake and energy homeostasis.

We hypothesized that the hypothalamic AMPK-fatty acid synthetic pathway is activated by peripheral administration of T3. T3 may cause an increase in hypothalamic AMPK activity, which in turn contributes to the development of T3-induced hyperphagia. The aim of this study is to elucidate the role of the AMPK-fatty acid synthetic pathway in food intake in T3-treated rats. We investigated the role of hypothalamic AMPK and acetyl-CoA carboxylase (ACC) phosphorylation in promoting the increase in food intake in T3-treated rats. Furthermore, we tested the central administration of compound C, a selective inhibitor of AMPK, in T3-treated rats to determine whether the AMPK-

Abbreviations: ACC, acetyl-CoA carboxylase; AGRP, agouti-related protein; AMPK, AMP-activated protein kinase; BAT, brown adipose tissue; CPT-1, carnitine palmitoyltransferase-1; D1, *deiodinase 1*; i.c.v., intracerebroventricular; i.p., intraperitoneal; NPY, neuropeptide Y; POMC, pro-opiomelanocortin; s.c., subcutaneous; STZ, streptozotocin; T3, triiodothyronine; T4, thyroxin; TRH, thyroid stimulating hormone-releasing hormone; TSH, thyroid stimulating hormone.

* Corresponding author. Tel.: +81 3 3822 2131; fax: +81 3 5685 1793.
E-mail address: shinya@nms.ac.jp (S. Ishii).

0167-0115/$ – see front matter © 2008 Elsevier B.V. All rights reserved.
doi:10.1016/j.regpep.2008.07.007

fatty acid synthetic pathway contributes to the increased food intake in T3-treated rats.

2. Materials and methods

2.1. Animal care and maintenance

Male Sprague Dawley rats (240–260 g; Saitama Experimental Animal Supply Co. Ltd., Saitama, Japan) were housed in air-conditioned animal quarters, with lights on between 0800 and 2000 h, and were given food and water *ad libitum*. The experiments were conducted according to the principles and procedures outlined in the NIH Guide for the Care and Use of Laboratory Animals. The protocol was approved by the Nippon Medical School Animal Care Research Committee.

2.2. Preparation of T3 for peripheral administration

T3 was prepared as 3,3',5-triiodo-L-thyronine (T3) (4.5 nmol/kg; Aldrich Chemical Co., Milwaukee, WI) dissolved in 5 mM NaOH. Control rats received a parallel injection with an equal volume of 5 mM NaOH. In the study of the acute effects of T3 on food intake, animals received a s.c. injection of either T3 (4.5 nmol/kg) or the vehicle (5 mM NaOH) ($n=7$ per group). Food, body weight and adiposity were weighed at 2-h and 4-h post-injection. In separate study, animals were killed by decapitation after 2-h post-injection for collection of trunk blood as described ($n=7$) [5]. In the chronic study, animals ($n=7$ per group) were given a s.c. injection of T3 or the vehicle daily for 6 days. Food intake and body weight were measured daily. On day 6, animals were decapitated after 2-h post-injection of T3. Trunk blood was collected on day 6 and the plasma was separated by centrifugation and stored at −80 °C until assayed. The hypothalami were dissected as previously described [10] and both were stored at −80 °C until assayed. Epididymal, retroperitoneal and inguinal fat pads, and interscapular brown adipose tissue (BAT) were dissected and weighed. Brains were removed and the hypothalami were snap frozen for subsequent measurement of neuropeptide mRNA expression by Northern blot and Western blot analyses (see below).

2.3. Intracerebroventricular cannulation

The animals were anesthetized with an i.p. injection of a mixture of Ketalar (ketamine HCl, 60 mg/kg; Pfizer, Tokyo, Japan) and Rompun (xylazine, 12 mg/kg; Bayer, Tokyo, Japan), and a 23-gauge stainless-steel cannula was implanted into the right lateral ventricle using a stereotaxic apparatus as previously described [10]. The upper incisor bar was set 3.3 mm below the interauricular line, and bregma was taken as A-P zero. The cannula tip was placed at A − 0.9, L − 1.2 and V − 3.6 mm and secured in place with dental acrylic. Only those rats whose cerebrospinal fluid overflowed through the cannula were used for the experiment. They were kept in individual cages and habituated by handling every day. Injections of the peptide were performed 10 days after placement of the cannula. Compound C (100 nmol in 10 μl of RPMI1640 [RPMI; Invitrogen, Carlsbad, CA]) was a gift from Merck & Co., Inc. (Whitehouse Station, NJ) [11]. In the acute study, compound C or vehicle (RPMI) was injected intracerebroventricularly (i.c.v.) just before s.c. treatment with T3. In the chronic study, compound C or RPMI was injected i.c.v. every 24 h for 6 days to control and T3-treated rats, and food intake was determined. Rats were treated 1 h before the onset of the dark cycle with either the vehicle or compound C in the chronic study.

2.4. RNA extraction and Northern blot analysis

Total tissue RNA was extracted with the TRizol reagent (Life Technologies, Inc., Gaithersburg, MD). The protocol for Northern blot analysis has been described previously [12,13]. Briefly, samples (10–20 μg of RNA per lane) were electrophoresed through a 1.5% agarose gel containing 2.2 M formaldehyde, and then transferred by capillary blotting onto a nylon membrane (Hybond-N+, Amersham Biosciences, Piscataway, NJ). Membrane blots were prehybridized in 1 M NaPO4, 20% SDS and 0.1% BSA for 2 h at 65 °C. 32P-Labeled specific riboprobes for NPY, agouti-related protein (AGRP), POMC or β-actin were added and the membranes were hybridized overnight at 65 °C. The membranes were washed at 65 °C in 2X SSC for 30 min; 2X SSC and 0.1% SDS for 30 min; and 0.5X SSC and 0.1% SDS for 30 min, and then exposed to Kodak XAR film at −70 °C for either 72 h for NPY and POMC, or 24 h for β-actin. The hybridization signal was determined from the autoradiograms using an NIH image analysis system.

2.5. Western blot analysis

In separate experiments, another pair of hypothalami were homogenized in lysis buffer (50 mM Tris–HCl [pH 7.5], 250 mM sucrose, 5 mM sodium pyrophosphate, 50 mM NaF, 1 mM EDTA, 1 mM dithiothreitol, 0.5 mM phenylmethylsulfonyl fluoride, 0.1 mM benzamidine, 50 μg/ml leupeptin, and 50 μg/ml soybean trypsin inhibitor). Protein concentration was determined with the DC protein assay (Bio-Rad Laboratories, Hercules, CA). The samples (40 μg) were mixed with 2X Laemmli sample buffer and then SDS was added to a final concentration of 0.2%. The lysates were boiled for 5 min, size separated on 4–15% Tris–HCl SDS Ready Gels (Bio-Rad Laboratories), and electrophoretically transferred to Hybond enhanced chemiluminescence nitrocellulose membranes (ECL, Amersham Biosciences). The blots were blocked in 5% nonfat dry milk (wt/vol) dissolved in phosphate-buffered saline containing 0.1% Tween 20 (PBS-T) and then washed four times for 5 min each in PBS-T. The blots were incubated overnight with primary antibodies against phospho-AMPKα (α1 and α2, Thr^{172}) (1:1000; Cell Signaling, Danvers, MA), phospho-ACC (Ser^{79}) (1:1000, Cell Signaling), anti-ACC (ACC1, 1:1000; Upstate Biotechnology, Lake Placid, NY) and anti-AMPKα (1:1000; Cell Signaling) in PBS-T and 5% BSA. The blots were washed and incubated with horseradish peroxidase-conjugated goat anti-rabbit IgG for phospho-AMPK α, AMPKα, phospho-ACC, and ACC (Amersham Biosciences; 1:20,000 dilution in PBS-T) for 1 h, washed again and then exposed for 1 min to the ECL Western Blotting Detection Reagent (Amersham Biosciences). Blots were exposed to Hyperfilm ECL (Amersham Biosciences) and developed. The films were developed, scanned and the image was analyzed using an NIH image analysis system.

2.5.1. Plasma hormone measurements

Plasma leptin [13], T3, thyroxin (T4), and thyroid stimulating hormone (TSH) [5] were measured with radioimmunoassays as previously described. Plasma desacyl and acyl ghrelin were measured with an ELISA (SCETI, Tokyo, Japan).

2.6. Data analysis

All data are presented as the mean ± SEM. Statistical analyses were carried out using an ANOVA, with the *post hoc* Fisher's Least Significant Difference method or an unpaired *t*-test (SigmaStat Ver. 3.5; Systat Software, Inc., Richmond, CA). $P<0.05$ was considered significant.

3. Results

3.1. Acute effects of T3 injection on food intake and plasma hormones

To examine the acute effect of T3 on food intake, rats received a single injection of T3. Two hours after the s.c. injection of T3, food intake increased (2.5 ± 0.5 [T3] vs. 0.4 ± 0.8 g [control], $P<0.05$) (Fig. 1A). The orexigenic effect of T3 was time-dependent and was no longer evident when assessed at 4 h after the administration of T3 (2.7 ± 1.1 [T3] vs. 0.5 ± 0.9 g [control]). There was no difference in body weight

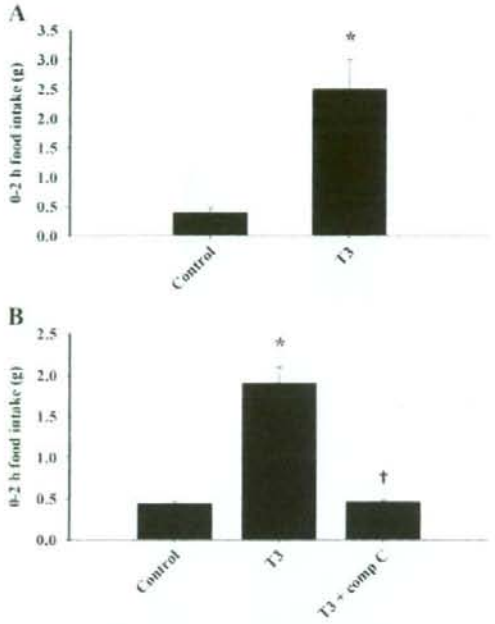

Fig. 1. Peripheral administration of T3 increases food intake. Rats fed *ad libitum* received a single s.c. injection of 4.5 nmol/kg T3 or the vehicle (control) ($n=7$ animals/group). Food intake was monitored (A). Food intake is affected by acute i.c.v. treatment with compound C. Male rats ($n=7$ animals/group) received a s.c. injection of an equal volume of 5 mM NaOH with or without T3, and food intake was monitored. Rats received an i.c.v. injection of 10 μl of saline with or without compound C (100 nmol/rat), and food intake was monitored (B). The results are the mean±SEM. *, $P<0.05$ vs. the control group, †, $P<0.05$, compared to the T3-treated group.

and adiposity after the acute treatment with T3. Plasma leptin levels were unchanged 2 h following T3 treatment (2.8±0.5 [T3] vs. 3.7±0.6 ng/ml [control]). However, plasma T3 was higher in the T3-treated group compared to the control group (4.2±1.1 [T3] vs. 1.2±0.1 ng/ml [control], $P<0.001$), but was still within the normal range. There was no difference in plasma T4 (4.0±0.4 [T3] vs. 3.8±0.2 μg/dl [control]) or TSH (1.8±0.8 [T3] vs. 1.3±0.3 ng/ml [control]) in the T3-treated animals compared to the controls.

3.2. Chronic effects of T3 injection on food intake, body weight and body adiposity

To determine the more chronic effects of T3, rats received 6 daily s.c. injections of T3 or the vehicle. At the end of the experiment, food intake significantly increased in the T3-treated rats compared to the vehicle-treated controls (Fig. 2A). There was no difference in body weight and adiposity after the chronic treatment with T3. Plasma leptin levels were unchanged after 6 daily injections of T3 (3.5±0.3 [T3] vs. 4.5±0.4 ng/ml [control]). Plasma T3 levels did not change in the T3-treated group compared to the control group (1.3±0.9 [T3] vs. 0.8±0.1 ng/ml [control]). There was no difference in plasma T4 (3.7±0.2 [T3] vs. 4.0±0.3 μg/dl [control]) or TSH (1.4±0.5 [T3] vs. 3.4±0.8 ng/ml [control]) in the T3-treated rats compared to the control rats.

3.3. Effects of acute and chronic T3 treatment on the expression of hypothalamic neuropeptides mRNAs

Following a single injection of T3, hypothalamic NPY mRNA levels (102±3.0% [T3] vs. 100±2.6% [control]), hypothalamic AGRP mRNA (106±5.2% [T3] vs. 100±4.4% [control]) or hypothalamic POMC mRNA levels (104±6.2% [T3] vs. 100±9.7% [control]) were unchanged compared to the control animals. This was also true for 6 daily injections of T3. Following 6 daily injections of T3, hypothalamic NPY mRNA levels (99±10.1% [T3] vs. 100±7.2% [control]), hypothalamic AGRP mRNA (108±9.5% [T3] vs. 100±5.7% [control]) or hypothalamic POMC mRNA levels (98±3.9% [T3] vs. 100±3.3% [control]) were unchanged compared to the control animals.

3.4. Acute effects of T3 on phosphorylation of hypothalamic AMPK and ACC

Fig. 3 shows the acute effects of T3 on the phosphorylation of hypothalamic AMPK and ACC. We determined the effect of T3 treatment on the levels of phosphorylation of the α1 and α2 catalytic subunits [14] of AMPK in the hypothalamus, which correlates with its activity. A single injection of T3 increased the levels of phosphorylated AMPK in the hypothalamus compared to the levels of phosphorylated AMPK in the vehicle-treated control animals (169±10.2% [T3] vs. 100±4.2% [control], $P<0.05$; Fig. 3A). A single injection of T3 also increased the levels of phosphorylated ACC in the hypothalamus (194±19.0% [T3] vs. 100±6.4% [control], $P<0.05$; Fig. 3B).

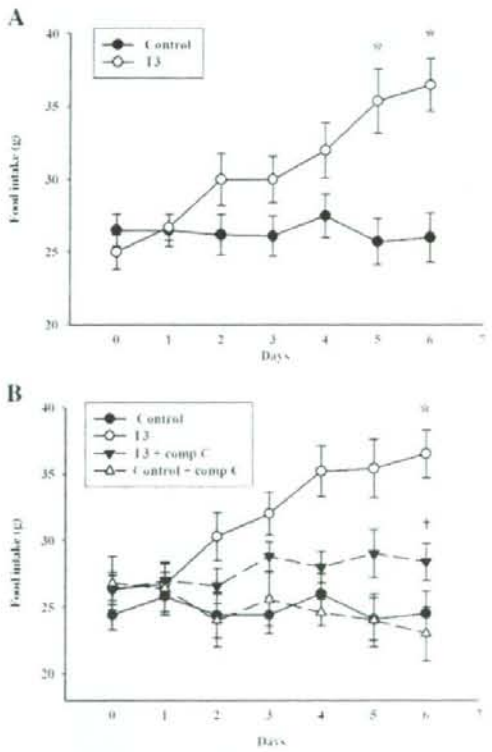

Fig. 2. Changes in daily food intake in rats. Male rats ($n=7$ animals/group) received a s.c. injection of an equal volume of the vehicle (5 mM NaOH) with or without T3. The data represent the mean±SEM ($n=7$ animals/group) (A) and effect chronic treatment with compound C in the T3-treated hyperphagic rat. Changes in daily food intake in rats injected i.c.v. with compound C (100 nmol/rat). Both control and T3-treated rats were injected i.c.v. with an equal volume of RPMI as the vehicle (B). The data represent the mean±SEM ($n=7$ animals/group). *, $P<0.05$ vs. the control group; †, $P<0.05$, compared to the T3-treated group.

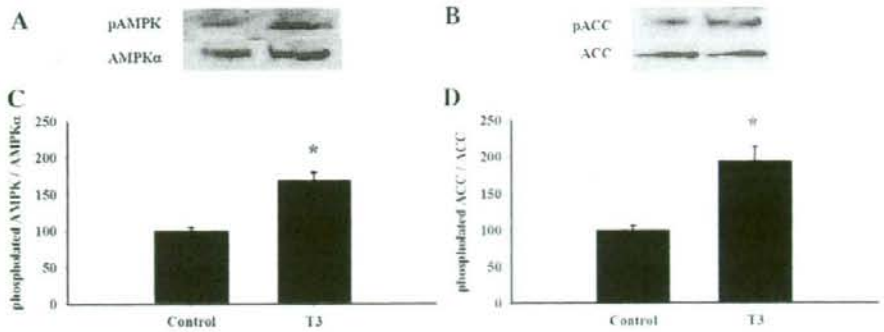

Fig. 3. Effects of acute treatment with T3 in rats on phosphorylation of hypothalamic AMPK and ACC. Representative Western blots of phosphorylated AMPK (pAMPK) and unphosphorylated AMPK (AMPKα) (A), and phosphorylated ACC (pACC) and unphosphorylated ACC (ACC) (B) in extracts of the hypothalamus. The average levels of pAMPK and pACC in the hypothalamus after a single s.c. injection of T3 are expressed as pAMPK/AMPKα (C) and pACC/ACC (D), respectively. The data, which are expressed as a percent of the control group, represent the mean ± SEM ($n = 7$ animals/group). *, $P < 0.05$, compared to the control group.

3.4.1. Chronic effects of T3 on phosphorylation of hypothalamic AMPK and ACC

Fig. 4 shows the chronic effect of 6 daily s.c. injections of T3 or the vehicle. T3 increased the levels of phosphorylated AMPK in the hypothalamus compared to the vehicle-treated controls (278 ± 33.3% [T3] vs. 100 ± 12.4% [control], $P < 0.01$; Fig. 4A). T3 also increased the levels of phosphorylated ACC in the hypothalamus (335 ± 45.4% [T3] vs. 100 ± 16.8% [control], $P < 0.01$; Fig. 4B).

3.5. Acute administration of compound C reserves the orexigenic effect of T3

To determine whether the enhanced hypothalamic AMPK activity is the cause of T3-induced hyperphagia, compound C, an AMPK inhibitor [11], was administered i.c.v. (100 nmol/rat) to the T3-treated rats. Animals that received the T3 treatment had a significantly increased food intake at 2 h compared to the vehicle-treated animals. Treatment with compound C significantly reversed the effect of the treatment with T3 on food intake (1.9 ± 0.2 [RPMI/T3], 0.46 ± 0.02 [compound C/T3], $P < 0.05$, RPMI/T3 vs. control, Fig. 1B). At 2-h post-injection of T3, there was no difference in food intake between the vehicle (NaOH)-treated compound C administered rats [compound C/NaOH] and the control animals [RPMI/NaOH] (0.4 ± 0.02 [RPMI/NaOH], 0.45 ± 0.04 [compound C/NaOH]). Plasma T3 was elevated in T3-treated RPMI administered animals and T3-treated compound C administered animals compared to control animals (4.1 ± 1.2 [RPMI/T3], 3.9 ± 0.9 [compound C/T3], 1.2 ± 0.1 ng/ml [control], $P < 0.001$, RPMI/T3 vs. control, compound C/T3 vs. control). However, T3 levels were still within the normal range among the three groups. There was no difference in the plasma levels of desacly ghrelin (136.5 ± 40.1 [RPMI/T3], 148.1 ± 26.3 [compound C/T3], 303.6 ± 70.5 pg/ml [control]). In addition, there was no difference in plasma levels of acyl ghrelin (149.0 ± 34.3 [RPMI/T3], 116.0 ± 17.9 [compound C/T3], 161.5 ± 9.5 pg/ml [control]). There was no difference in the plasma levels of T4, leptin, and TSH in the T3-treated rats compared to the control rats.

3.6. Chronic administration of compound C reserves the orexigenic effect of T3

There was no difference in daily food intake between the compound C administered control animals [compound C/NaOH] and control animals [RPMI/NaOH]. At 6 days post-injection, there was no difference in body weight among the three treated groups (Table 1). Chronic treatment with T3 did not change the plasma levels of T3, T4, leptin, TSH, desacyl ghrelin or acyl ghrelin. Chronic administration of

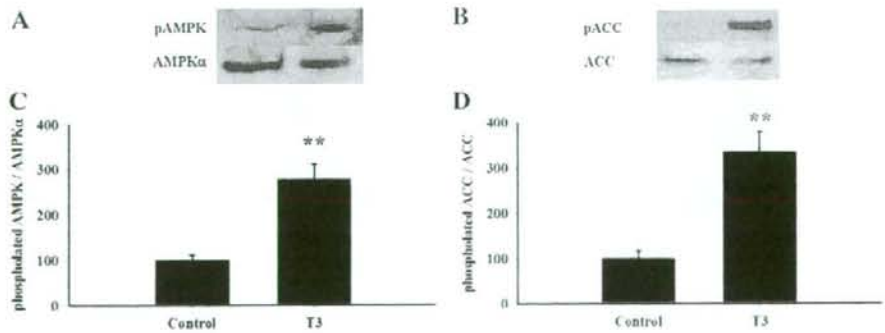

Fig. 4. Effects of chronic treatment with T3 in rats on phosphorylation of hypothalamic AMPK and ACC. Representative Western blots of phosphorylated AMPK (pAMPK) and unphosphorylated AMPK (AMPKα) (A), and phosphorylated ACC (pACC) and unphosphorylated ACC (ACC) (B) in extracts of the hypothalamus. The average levels of pAMPK and ACC in the hypothalamus after multiple s.c. injections of T3 are expressed as pAMPK/AMPKα (C) and pACC/ACC (D), respectively. The data, which are expressed as a percent of the control group, represent the mean ± SEM ($n = 7$ animals/group). **, $P < 0.01$, compared to the control group.

Table 1
Comparisons of food intake, body weight, fat weight, plasma T3, plasma T4, plasma TSH, and various adipose tissue weights in rats treated with T3 plus compound C (comp C) or the vehicle for 6 days

	Control	T3	T3 + comp C
Initial Food intake (g/24 h)	26.4±1.1	26.9±0.9	26.7±1.3
Final Food intake (g/24 h)	24.5±1.2	29.6±0.8*	25.2±1.1
Final body weight (g)	377±7.8	370±9.4	362±9.0
ΔBody weight (g)	20±1.1	14±3.0	6±0.5
Epididymal fat weight (g)	3.9±0.5	3.2±0.4	3.3±0.4
Retroperitoneal fat weight (g)	3.1±0.6	2.0±0.5	2.4±0.7
Inguinal fat weight (g)	3.0±0.3	2.8±0.3	2.9±0.3
BAT weight (g)	1.7±0.2	1.9±0.2	1.6±0.2
Plasma leptin (ng/ml)	4.5±0.4	3.5±0.3	4.0±0.6
Plasma T3 (ng/ml)	1.1±0.1	1.7±0.2	0.7±0.1
Plasma T (ng/ml)	4.6±0.4	1.7±0.3	1.8±0.2
Plasma TSH (ng/ml)	3.4±1.2	1.0±0.3	0.8±0.2
Plasma desacyl ghrelin (pg/ml)	252.5±69.2	114.5±21.5	91.7±21.6
Plasma acyl ghrelin (pg/ml)	182.3±47.4	197.5±19.5	189.3±50.5

Rats fed *ad libitum* were injected s.c. once daily with 4.5 nmol/kg T3 or the vehicle. Compound C or RPMI 1640 was injected i.c.v. every 24 h for 6 days to the control and T3-treated rats ($n=7$ animals/group). The results are the mean±SEM.
*, $P<0.05$, vs. the control group.

T3 did not alter epididymal fat, retroperitoneal fat, subcutaneous fat, and BAT weight (Table 1).

4. Discussion

In the present study, we used a substantially lower dose of T3 than the dose used in our earlier study to determine whether hypothalamic AMPK plays an important role in the regulation of food intake. We previously showed that T3-treated rats are markedly hyperphagic. The decreased plasma leptin levels could contribute to the hyperphagia in T3-induced thyrotoxicosis associated with increased hypothalamic NPY and decreased hypothalamic POMC gene expression [3]. However, recently Kong et al. [4] reported that the dose of T3 (4.5 nmol/kg) that was used in our study could stimulate food intake independently of plasma leptin levels, and did not change either hypothalamic NPY or hypothalamic POMC gene expression. Consistent with the report by Kong et al., in the present study, rats that received a single injection of T3 had increased food intake without alterations in NPY, AGRP and POMC mRNA levels, but did have increased hypothalamic phosphorylated AMPK and hypothalamic phosphorylated ACC. To determine the more chronic effects of T3, rats received 6 daily s.c. injections of T3 or vehicle. Although food intake increased without significant alterations in plasma leptin levels or in hypothalamic NPY, AGRP or POMC mRNA levels, multiple T3 injections did increase hypothalamic phosphorylated AMPK and phosphorylated ACC. Furthermore, we demonstrated that compound C, an AMPK inhibitor, administered i.c.v. effectively blocked the food intake induced by a single or multiple injections of T3. These data suggest that hypothalamic AMPK plays an important role in the regulation of food intake in T3-treated rats. In this study, we showed an increased food intake in rats but human studies have not proven a role for T3 in appetite regulation. Martin et al. reported that low oral doses of T3 did not increase food intake in humans; however, they discussed the possibility that oral T3 administration may not be directly comparable to subcutaneous injection of T3 [15]. They also indicated that their study was small and was underpowered to detect small differences in food intake. Thus, their data do not contradict our results that low doses of T3 increased food intake in rats.

AMPK is known as the rate-limiting enzyme for the synthesis of ACC. ACC stimulates the conversion acetyl-CoA to malonyl-CoA. AMPK activation is known to decrease ACC activity by phosphorylation [16,17]. Thus, malonyl-CoA levels were decreased by the increased phosphorylated ACC, which has been hypothesized to act as an inhibitor of feeding. Alternatively, decreased malonyl-CoA levels stimulated carnitine palmitoyltransferase-1 (CPT-1) activity [18]. Increased CPT-1 activity has been reported to stimulate food intake [19]. However, we did not measure AMPK activity. It has been reported that phosphorylation of a subunit of AMPK correlates with its activity [11]. Several lines of evidence demonstrated that AMPK plays an important role in the regulation of food intake. It has been reported that fasting increases hypothalamic AMPK activity, whereas refeeding inhibits its activity [20]. In the present study, we reported that T3-treated rats did not have decreased plasma leptin levels. The orexigenic peptides, cannabinoids and ghrelin, stimulate hypothalamic AMPK activity [21]. A recent study showed that hypothalamic AMPK activity was elevated in streptozotocin (STZ)-treated rats. Furthermore, compound C, a specific AMPK inhibitor, effectively blocked STZ-induced hyperphagia [22]. We previously reported that plasma ghrelin was elevated in STZ-induced hyperphagic rats [10]. Unfortunately, there was no change in plasma desacyl and acyl ghrelin in T3-treated animals in the acute or chronic study. How T3 activates hypothalamic AMPK activity is largely unknown. Kong et al. [4] reported that low doses of T3 injected directly into the hypothalamic ventromedial nucleus increase food intake. In addition, plasma T3 easily crosses the blood-brain barrier. We speculate that T3 directly stimulates hypothalamic AMPK phosphorylation. There is also evidence suggesting that during fasting locally produced T3 in the arcuate nucleus might increase rebound feeding associated with fasting, possibly through UCP-2 [23]. Coppola et al. reported that fasting increased type 2 diiodinase activity and local thyroid hormone production in the arcuate nucleus. They also showed that fasting increased T3 mediated UCP-2 activation resulting in mitochondrial proliferation in NPY/AGRP neurons. Further studies will be needed to determine whether UCP-2 regulates hypothalamic AMPK activity. In this study, we demonstrated that i.c.v. injection of compound C significantly blocked the food intake induced by either a single or multiple injections of T3. These data support the suggestion that the increase in food intake induced by T3 is closely associated with an increase in the activity of AMPK.

In the present study, there was no difference in plasma T4, TSH, and leptin levels in acute T3-treated rats compared to control rats; however, plasma T3 levels were higher in the T3-treated group than in the control group, but they remained within the normal range. Furthermore, there was no difference in plasma T3, T4, TSH, and leptin levels in chronic T3-treated rats compared to control rats. Consistent with the report by Kong et al., we performed these experiments very carefully because excess T3 would suppress plasma T4 and TSH. These data support the contention that suppressed plasma leptin levels did not contribute to the development of T3-induced hyperphagia in the present study.

Chronic injection of T3 results in a significant increase in food intake, yet the body weight does not appear to increase (Table 1) and there are no large differences in T3 or T4 levels between T3-treated and vehicle-treated rats. Like the acute study, we did not find markedly increased T3 levels in the chronic study. The enzyme 5'-iodothyronine deiodinase is responsible for the metabolism of T4 to T3. In rats, type 1 deiodinase (D1) is predominantly found in the liver, kidney and thyroid gland. It has been reported that TSH increases D1 activity. We speculate that chronic administration of T3 suppressed T4, TSH and D1 activity. Suppressed T4 levels and D1 activity caused a decrease in endogenous T3 levels. Thus, T3 levels were not elevated as in the acute study. We reported that there is no large difference in body weight between T3-treated animals and vehicle-treated animals in this study. We speculate that an increase in food intake promotes accumulation in adipose tissue in T3-treated animals. On the other hand, T3 has lypolytic effects to adipose tissue. These mechanisms could explain why there was no big change in body weight despite the excessive food intake in the T3-treated rats.

Several lines of evidence demonstrate that hypothalamic thyroid hormone-releasing hormone (TRH) regulates food intake. It has been reported that fasting reduced TRH gene expression. Furthermore, TRH treatment decreased food intake [24]. On the other hand, the POMC-deficient mouse shows increased food intake and becomes obese, and

the TRH content of these mice does not differ from that of control mice [25]. These data suggest that hypothalamic TRH does not contribute to the development of the hyperphagia in the POMC-deficient mouse. In this study, we did not measure TRH mRNA, and the T3 treatment may have reduced TRH mRNA. Thus, suppressed hypothalamic TRH mRNA might stimulate food intake in T3-treated rats. It has been reported that there are nongenomic effects of thyroid hormone in various tissues [26]. The nongenomic actions of T3 have been shown to rapidly shorten action potential duration in rat ventricular myocytes [27]. The nongenomic effects may occur within seconds or minutes. These data indicated that thyroid hormone regulates enzyme production at a pre-translational level. In this regard, the stimulation of food intake by T3 in the present study might be due to a genomic effect. Additional studies are needed to determine whether these stimulatory actions on food intake by thyroid hormone are genomic or nongenomic.

In summary, the present study has demonstrated that both acute and chronic injections of T3 enhance hypothalamic AMPK and ACC phosphorylation. Compound C, an AMPK inhibitor, effectively blocked the food intake induced by both single and multiple injections of T3. Taken together, these results support the hypothesis that activation of hypothalamic AMPK plays an important role in regulating food intake in low-dose T3-treated rats.

Acknowledgments

This works was supported in part by a Grant-in-Aid for scientific research from the Japanese Ministry of Education, Science and Culture *to J.K.* (KAKENHI 17590970) and a Grant from the Hakujikai, Institute of Gerontology to J.K. We thank Dr. T. Shimokawa (Astellas Pharma Inc.) for his helpful suggestions. The authors also acknowledge Mrs. M. Kawahara for her technical assistance.

References

[1] Oppenheimer JH, Schwartz HL, Lane JT, Thompson MP. Functional relationship of thyroid hormone-induced lipogenesis, lipolysis, and thermogenesis in the rat. J Clin Invest 1991;87:125–32.
[2] Abraham G, Falcou R, Rozen R, Mandenoff A, Autissier N, Apfelbaum M. The effects of a constant T3 level and thermoneutrality in diet-induced hyperphagia. Horm Metab Res 1987;19:96–100.
[3] Ishii S, Kamegai J, Tamura H, Shimizu T, Sugihara H, Oikawa S. Hypothalamic neuropeptide Y/Y1 receptor pathway activated by a reduction in circulating leptin, but not by an increase in circulating ghrelin, contributes to hyperphagia associated with triiodothyronine-induced thyrotoxicosis. Neuroendocrinology 2003;78:321–30.
[4] Kong WM, Martin NM, Smith KL, Gardiner JV, Connoley IP, Stephens DA, et al. Triiodothyronine stimulates food intake via the hypothalamic ventromedial nucleus independent of changes in energy expenditure. Endocrinology 2004;145:5252–8.
[5] Kim MS, Park JY, Namkoong C, Jang PG, Ryu JW, Song HS, et al. Anti-obesity effects of alpha-lipoic acid mediated by suppression of hypothalamic AMP-activated protein kinase. Nat Med 2004;10:727–33.
[6] Minokoshi Y, Alquier T, Furukawa N, Kim YB, Lee A, Xue B, et al. AMP-kinase regulates food intake by responding to hormonal and nutrient signals in the hypothalamus. Nature 2004;428:569–74.
[7] Andersson U, Filipsson K, Abbott CR, Woods A, Smith K, Bloom SR, et al. AMP-activated protein kinase plays a role in the control of food intake. J Biol Chem 2004;279:12005–8.
[8] Hardie DG, Carling D. The AMP-activated protein kinase-fuel gauge of the mammalian cell? Eur J Biochem 1997;246:259–73.
[9] Hawley SA, Davison M, Woods A, Davies SP, Beri RK, Carling D, et al. Characterization of the AMP-activated protein kinase kinase from rat liver and identification of threonine 172 as the major site at which it phosphorylates AMP-activated protein kinase. J Biol Chem 1996;271:27879–87.
[10] Ishii S, Kamegai J, Tamura H, Shimizu T, Sugihara H, Oikawa S. Role of ghrelin in streptozotocin-induced diabetic hyperphagia. Endocrinology 2002;143:4934–7.
[11] Zhou G, Myers R, Li Y, Chen Y, Shen X, Fenyk-Melody J, et al. Role of AMP-activated protein kinase in mechanism of metformin action. J Clin Invest 2001;108:1167–74.
[12] Ishii S, Shibasaki T, Murakami T, Shima K, Wakabayashi I. Response of leptin mRNA to 24-h food deprivation and refeeding is influenced by age in rats. Regul Pept 2000;92:45–50.
[13] Kamegai J, Tamura H, Shimizu T, Ishii S, Sugihara H, Wakabayashi I. Chronic central infusion of ghrelin increases hypothalamic neuropeptide Y and agouti related protein mRNA levels and body weight in rats. Diabetes 2001;50:2438–43.
[14] Hawley SA, Davison M, Woods A, Davies SP, Beri RK, Carling D, et al. Characterization of the AMP-activated protein kinase kinase from rat liver and identification of threonine 172 as the major site at which it phosphorylates AMP-activated protein kinase. J Biol Chem 1996;271:27879–87.
[15] Martin NM, Small CJ, Lee JL, Ellis S, Dhillo WS, Smith KL, et al. Low-dose oral tri-iodothyronine does not directly increase food intake in man. Diabetes Obes Metab 2007;9:435–7.
[16] Munday MR, Carling D, Hardie DG. Negative interactions between phosphorylation of acetyl-CoA carboxylase by the cyclic AMP-dependent and AMP-activated protein kinases. FEBS Lett 1988;235:144–8.
[17] Carlson CA, Kim KH. Regulation of hepatic acetyl coenzyme A carboxylase by phosphorylation and dephosphorylation. J Biol Chem 1973;248:378–80.
[18] Saha AK, Kurowski TG, Ruderman NB. A malonyl-CoA fuel-sensing mechanism in muscle: effects of insulin, glucose, and denervation. Am J Physiol 1995;269:E283–9.
[19] Obici S, Feng Z, Arduini A, Conti R, Rossetti L. Inhibition of hypothalamic carnitine palmitoyltransferase-1 decreases food intake and glucose production. Nat Med 2003;9:756–61.
[20] Minokoshi Y, Alquier T, Furukawa N, Kim YB, Lee A, Xue B, et al. AMP-kinase regulates food intake by responding to hormonal and nutrient signals in the hypothalamus. Nature 2004;428:569–74.
[21] Kola B, Hubina E, Tucci SA, Kirkham TC, Garcia EA, Mitchell SE, et al. Cannabinoids and ghrelin have both central and peripheral metabolic and cardiac effects via AMP-activated protein kinase. J Biol Chem 2005;288:25196–201.
[22] Namkoong C, Kim MS, Jang PG, Han SM, Park HS, Koh EH, et al. Enhanced hypothalamic AMP-activated protein kinase activity contributes to hyperphagia in diabetic rats. Diabetes 2005;54:63–8.
[23] Coppola A, Liu ZW, Andrews ZB, Paradis E, Roy MC, Friedman JM, et al. Central thermogenic-like mechanism in feeding regulation: an interplay between arcuate nucleus T3 and UCP2. Cell Metab 2007;5:21–33.
[24] Vijayan E, McCann SM. Suppression of feeding and drinking activity in rats following intraventricular injection of thyrotropin releasing hormone (TRH). Endocrinology 1977;100:1727–30.
[25] Martin NM, Small CJ, Sajedi A, Liao XH, Weiss RE, Gardiner JV, et al. Abnormalities of the hypothalamo-pituitary-thyroid axis in the pro-opiomelanocortin deficient mouse. Regul Pept 2004;122:169–72.
[26] Davis PJ, Davis FB, Lawrence WD. Thyroid hormone regulation of membrane Ca2 (+)-ATPase activity. Endocr Res 1989;15:651–82.
[27] Sun ZQ, Ojamaa K, Coetzee WA, Artman M, Klein I. Effects of thyroid hormone on action potential and repolarizing currents in rat ventricular myocytes. Am J Physiol 2000;278:E302–7.

Biosci. Biotechnol. Biochem., **72** (8), 2210–2213, 2008

Note

Validation of an Ion Trap Tandem Mass Spectrometric Analysis of Mulberry 1-Deoxynojirimycin in Human Plasma: Application to Pharmacokinetic Studies

Kiyotaka NAKAGAWA,[1,†] Hiroyuki KUBOTA,[1] Tsuyoshi TSUZUKI,[1] Jun KARIYA,[2] Toshiyuki KIMURA,[3] Shinichi OIKAWA,[4] and Teruo MIYAZAWA[1]

[1]*Food and Biodynamic Chemistry Laboratory, Graduate School of Agricultural Science, Tohoku University, Sendai 981-8555, Japan*
[2]*Project M Co., Ltd., Sendai 980-0845, Japan*
[3]*National Agricultural Research Center for Tohoku Region, Fukushima 960-2156, Japan*
[4]*Department of Medicine, Nippon Medical School, Tokyo 113-8603, Japan*

Received April 1, 2008; Accepted May 8, 2008; Online Publication, August 7, 2008
[doi:10.1271/bbb.80200]

Mulberry 1-deoxynojirimycin (DNJ) is a potent α-glucosidase inhibitor. Although it is useful for the treatment of diabetes, the human absorption and metabolism of DNJ have never been characterized. We developed a method using hydrophilic interaction chromatography coupled with ion trap tandem mass spectrometry, and found that orally administered DNJ was absorbed into the blood and then excreted into the urine.

Key words: mulberry; 1-deoxynojirimycin; tandem mass spectrometry; absorption; human plasma

According to the Japanese Health, Labor and Welfare Ministry, there are over 7 million Japanese people with diabetes, and this number has been increasing in recent years. On the other hand, Japanese mulberry sericulture (the silkworm industry) was once among the biggest such industry in the world, but has long been in decline due to cheaper imported silk. Related to these factors, the practical use of azasugar 1-deoxynojirimycin (DNJ, an intestinal α-glucosidase inhibitor present in mulberry leaves) has gained considerable attention for its potential as a functional or medical food to control blood glucose, thereby preventing diabetes and also promoting a revival of sericulture.[1,2]

While DNJ inhibits α-glucosidase activity, the concentration of the compound in most commercial mulberry leaf products is as low as about 0.2 percent.[3] We recently produced a food-grade mulberry extract with a high DNJ content (about 0.5–3 percent) from young mulberry leaves. We then recruited healthy volunteers, and determined the effective dose of the mulberry extract needed to suppress the elevation of postprandial blood glucose and the secretion of insulin.[4] The results revealed the human physiological impact of mulberry DNJ, and the antihyperglycemic effect is now being further investigated in diabetic patients as well as overweight subjects who are more susceptible to the disease.

Anticipating the future use of mulberry DNJ by the food industry, it has become important to elucidate its absorption and metabolism in humans from the point of view of food safety. However, the metabolic fate of orally administered mulberry DNJ has not been characterized, except in our recent rat study.[5] In that study, to evaluate the metabolic disposition, we developed a hydrophilic interaction chromatographic method coupled with mass spectrometric detection (HILIC-MS). This allowed us to show the occurrence of orally administered mulberry DNJ in rat plasma. When rats received mulberry DNJ (110 mg/kg of body weight), DNJ reached a concentration of 1500 ng/ml in the plasma. However, we were unable to detect DNJ in human samples by HILIC-MS, because of its limited sensitivity. We now report direct evidence for the rapid absorption and elimination of mulberry DNJ in humans which was achieved by both a new DNJ extraction method using an internal standard (miglitol) and a newly developed analytical procedure using HILIC with hybrid quadrupole/linear ion trap tandem mass spectrometry (QTRAP MS/MS).

Two male subjects aged 23–24 years participated in this study, and gave written informed consent to the experimental protocol which was approved by the ethics committee of Nippon Medical School. These subjects

† To whom correspondence should be addressed. Fax: +81-22-717-8905; E-mail: nkgw@biochem.tohoku.ac.jp

Abbreviations: DNJ, 1-deoxynojirimycin; HILIC, hydrophilic interaction chromatography; MRM, multiple reaction monitoring; MS, mass spectrometer; MS/MS, tandem mass spectrometer; QTRAP, quadrupole/linear ion trap

orally consumed 1.2 g of the mulberry extract[4] containing 6.3 mg of DNJ after fasting overnight. The dose was equal to the amount needed to suppress the elevation of postprandial blood glucose in humans.[4] Before and 0.5–48 h after administration, blood samples were obtained in tubes containing heparin as an anticoagulant. Plasma was prepared by centrifugation at 1,600 × *g* for 10 min at 4 °C. Urine was collected during time periods 0–24 and 24–48 h after administration.

To the plasma (100 µl), 25 ng of an internal standard (miglitol; Toronto Research Chemicals, Toronto, Canada), 100 µl of water and 600 µl of acetonitrile were added and mixed by sonicating for 1 min and vortexing for 30 s. After centrifuging at 1600 × *g* for 15 min at 4 °C, the supernatant was collected and passed through a PTFE filter (0.45-µm pore size; Sartorius, Göttingen, Germany). A portion (5 µl) of the resulting extract was injected into the HILIC-QTRAP MS/MS apparatus as described later. In the case of urine (about 900 ml), it was adjusted to 1000 ml with water. The diluted urine (100 µl) was mixed with 25 ng of an internal standard, 100 µl of water and 600 µl of acetonitrile. After centrifuging, the supernatant was analyzed by HILIC-QTRAP MS/MS.

The HILIC-QTRAP MS/MS apparatus consisted of a liquid chromatograph (Shimadzu, Kyoto, Japan) and 4000 QTRAP MS/MS (Applied Biosystems, Foster City, CA, USA). Under positive ion electrospray ionization conditions, the QTRAP MS/MS parameters (*e.g.*, collision energy) were optimized with standard DNJ (Wako, Tokyo, Japan). The plasma and urine extracts (5 µl each) were separated in a HILIC column (TSK gel Amide-80, 2.0 mm × 150 mm; Tosoh, Tokyo, Japan),[3] eluted with a mixture of acetonitrile and water (675:325, v/v) containing 6.5 mM ammonium formate (pH 5.5) at a flow rate of 0.2 ml/min, and maintained at 40 °C. DNJ was detected in the post column by HILIC-QTRAP MS/MS with multiple reaction monitoring (MRM) for transition of the parent ion to the product ion. The concentrations of plasma and urine DNJ were calculated from a calibration curve for standard DNJ, and then corrected according to the recovery of the internal standard (miglitol) which averaged 70% for the plasma sample and 80% for the urine sample. The human administration trial was conducted twice, and the concentration data are expressed as the mean of the two trials.

The recently developed QTRAP MS/MS method offers specific benefits for biomolecular analysis.[6] With the advent of QTRAP MS/MS, product ion scanning and MRM provide useful structural information on the analytes, even in the presence of background contaminants from complex biological matrices. The analysis of some azasugars[7,8] and biomoleculars[9,10] by QTRAP MS/MS has recently been reported. A HILIC-MS/MS analysis of DNJ in mulberry leaves has been reported,[7] but the method has not been applied to the determination of DNJ in human samples. On the basis of this background, we developed this new method for determining DNJ by HILIC-QTRAP MS/MS to investigate the absorption and metabolism of orally administered mulberry DNJ in humans.

We first analyzed standard DNJ by using QTRAP MS/MS with flow injection. DNJ showed an intense molecular ion at m/z 164 $[M + H]^+$ in the Q1 mass spectrum. We then conducted product ion scanning with Q3 in the linear ion trap mode, and identified DNJ-specific fragment ions (*e.g.*, m/z 110 $[M + H\text{-}3H_2O]^+$) (Fig. 1A). Similarly, the QTRAP MS/MS parameters were optimized with miglitol (the internal standard). The DNJ- or miglitol-specific fragment ions allowed selective detection of the analytes by using HILIC-QTRAP MS/MS with MRM. In the MRM chromatogram (Fig. 1B), standard DNJ could be clearly detected at 6.7 min, together with miglitol at 6.4 min. The calibration curve for DNJ showed good linearity ($R^2 = 0.997$), and the detection limit was 20 pg/injection at a signal-to-noise ratio of 3. This detection limit is 25 times more sensitive than that with our previous HILIC-MS method.[5]

As shown in Fig. 1C, DNJ was not detected in the plasma extract taken before administering the mulberry extract (containing 6.3 mg of DNJ). However, 1 h after the oral administration, a clear peak ascribable to DNJ (6.7 min) was observed in the plasma extract, together with a peak of internal standard miglitol (6.4 min). These findings clearly indicate that orally administered mulberry DNJ was absorbed from the alimentary tract of humans. Our HILIC-QTRAP MS/MS method was satisfactorily selective and convenient enough for measuring DNJ present in human plasma. The high reproducibility for determining plasma DNJ (coefficient of variability < 5%) was confirmed and was not affected by storage of the plasma samples at −80 °C for 1 week. These results indicate the quantitative accuracy of the HILIC-QTRAP MS/MS method which would be a useful tool for studying the metabolic fate of mulberry DNJ, as well as its bioavailability.

Figure 1D shows the time-course characteristics of DNJ concentration in the plasma after an oral administration of the mulberry extract. The concentration of DNJ in the plasma increased to the highest level (520 ng/ml) 1.5 h after its administration and decreased thereafter. It is generally known that when humans received an effective dose of azasugars (*e.g.*, 50 mg of miglitol), the plasma concentration reached about 1300 ng/ml.[8] Considering the present dose (6.3 mg of DNJ), the plasma level of DNJ (Fig. 1D) seems to be roughly comparable to that of other azasugars. The bioactivity of DNJ in the digestive tract (α-glucosidase inhibition) has been thoroughly investigated,[1,2] although little attention has been paid to the effects of DNJ within the human body. Iizuka *et al.* have studied the antidiabetic effect of mulberry DNJ by using diabetic rats and revealed its unique properties of increasing insulin sensitivity.[11] Considering the human plasma

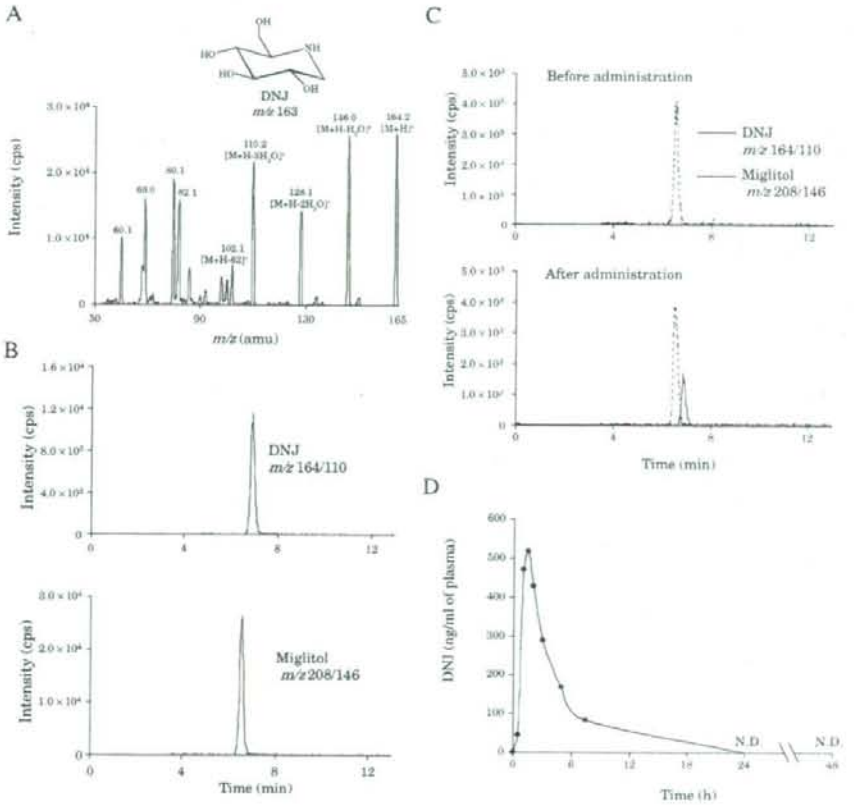

Fig. 1. Q3 Mass Spectrum (A) and Multiple Reaction Monitoring (MRM) Chromatograms (B and C) of Standard DNJ and Plasma Samples Collected from Human Subjects before and after the Administration of a Mulberry Extract Containing 6.3 mg of DNJ, and Time-Course Changes in Plasma DNJ Concentration (D).

A, Standard DNJ (500 ng/ml) was infused directly into the QTRAP MS/MS apparatus with a syringe pump at a flow rate of 0.01 ml/min, and product ion scanning for m/z 164 $[M+H]^+$ was performed; B, standard DNJ or miglitol (each 1 ng) was analyzed by HILIC-QTRAP MS/MS with MRM for transition of the parent ion (m/z 164 for DNJ and m/z 208 for miglitol) to the product ion (m/z 110 for DNJ and m/z 146 for miglitol); C and D, human plasma extract before and 1.5 h after the oral administration of mulberry DNJ (6.3 mg/human) was analyzed by HILIC-QTRAP MS/MS with MRM, and the plasma DNJ concentration was calculated.

concentration of DNJ (Fig. 1D), it is likely that DNJ may act as a bioactive compound within the body (*e.g.*, affecting the secretion of insulin). This possibility remains to be confirmed, so further studies are needed.

We finally investigated urine and detected DNJ (7.0 μg/ml) in the 0–24 h urine, implying that the majority of administered DNJ would be excreted in the urine. In support of this, DNJ in the 24–48 h urine was at a trace level (<0.5 μg/ml). On the basis of the present findings, we can speculate one possible metabolic fate of mulberry DNJ. The majority of orally administered mulberry DNJ is absorbed from the intestines into the portal vein. Since DNJ is structurally similar to glucose, the intestinal absorption of DNJ may be regulated *via* the glucose transporter.[12] The DNJ incorporated into the bloodstream is excreted into the urine. Since DNJ has a relatively short half-life, the tissue distribution and accumulation may not be particularly high. As for the metabolites of mulberry DNJ, there is a possibility that a small part of administered DNJ is metabolized by drug-metabolizing enzymes in the liver such as cytochrome P450s. Therefore, screening and structural characterization of DNJ metabolites are the subject of ongoing investigation.

In conclusion, although there have been several reports about the absorption and metabolic fate of azasugars in animals,[13–15] they have not provided any information about the intestinal absorption, metabolites, and pharmacokinetic profiles of orally administered mulberry DNJ in humans. We used in this study the newly developed HILIC-QTRAP MS/MS method to

demonstrate that orally administered mulberry DNJ was absorbed from the alimentary tract of a human and then excreted from the body. Considering the rapid elimination of DNJ from the body, it may lack side effects. Hence, mulberry DNJ might be therapeutically used as an effective food in the treatment of non-insulin-dependent diabetes mellitus, and future clinical study are required to evaluate the efficacy and safety concerning tissue distribution and the side effects of DNJ.

Acknowledgments

This work was supported by the Supporting Program for Creating University Ventures, Japan Science and Technology Agency.

References

1) Asano, N., Nash, R. J., Molyneux, R. J., and Fleet, G. W. J., Sugar-mimic glycosidase inhibitors: natural occurrence, biological activity and prospects for therapeutic application. *Tetrahedron: Asymmetry*, **11**, 1645–1680 (2000).
2) Mudra, M., Ercan-Fang, N., Zhong, L., Furne, J., and Levitt, M., Influence of mulberry leaf extract on the blood glucose and breath hydrogen response to ingestion of 75 g sucrose by type 2 diabetic and control subjects. *Diabetes Care*, **30**, 1272–1274 (2007).
3) Kimura, T., Nakagawa, K., Saito, Y., Yamagishi, K., Suzuki, M., Yamaki, K., Shinmoto, H., and Miyazawa, T., Determination of 1-deoxynojirimycin in mulberry leaves using hydrophilic interaction chromatography with evaporative light scattering detection. *J. Agric. Food Chem.*, **52**, 1415–1418 (2004).
4) Kimura, T., Nakagawa, K., Kubota, H., Kojima, Y., Goto, Y., Yamagishi, K., Oita, S., Oikawa, S., and Miyazawa, T., Food-grade mulberry powder enriched with 1-deoxynojirimycin suppresses the elevation of postprandial blood glucose in human. *J. Agric. Food Chem.*, **55**, 5869–5874 (2007).
5) Nakagawa, K., Kubota, H., Kimura, T., Yamashita, S., Tsuzuki, T., Oikawa, S., and Miyazawa, T., Occurrence of orally administered mulberry 1-deoxynojirimycin in rat plasma. *J. Agric. Food Chem.*, **55**, 8928–8933 (2007).
6) King, R., and Fernandez-Metzler, C., The use of Qtrap technology in drug metabolism. *Curr. Drug Metab.*, **7**, 541–545 (2006).
7) Nuengchamnong, N., Ingkaninan, K., Kaewruang, W., Wongareonwanakij, S., and Hongthongdaeng, B., Quantitative determination of 1-deoxynojirimycin in mulberry leaves using liquid chromatography-tandem mass spectrometry. *J. Pharm. Biomed. Anal.*, **44**, 853–858 (2007).
8) Li, X., Wang, Y., Wang, J., Fawcett, J. P., Zhao, L., and Gu, J., Determination of miglitol in human plasma by liquid chromatography/tandem mass spectrometry. *Rapid Commun. Mass Spectrom.*, **21**, 247–251 (2007).
9) Nakagawa, K., Oak, J. H., Higuchi, O., Tsuzuki, T., Oikawa, S., Otani, H., Mune, M., Cai, H., and Miyazawa, T., Ion trap tandem mass spectrometric analysis of Amadori-glycated phosphatidylethanolamine in human plasma with or without diabetes. *J. Lipid Res.*, **46**, 2514–2524 (2005).
10) Nakagawa, K., Ibusuki, D., Suzuki, Y., Yamashita, S., Higuchi, O., Oikawa, S., and Miyazawa, T., Ion-trap tandem mass spectrometric analysis of squalene monohydroperoxide isomers in sunlight-exposed human skin. *J. Lipid Res.*, **48**, 2779–2787 (2007).
11) Iizuka, Y., Sakurai, E., and Tanaka, Y., Antidiabetic effect of *folium mori* in GK rats. *Yakugaku Zasshi* (in Japanese), **121**, 365–369 (2001).
12) Voss, A. A., Diez-Sampedro, A., Hirayama, B. A., Loo, D. D., and Wright, E. M., Imino sugars are potent agonists of the human glucose sensor SGLT3. *Mol. Pharmacol.*, **71**, 628–634 (2007).
13) Faber, E. D., Oosting, R., Neefjes, J. J., Ploegh, H. L., and Meijer, D. K., Distribution and elimination of the glycosidase inhibitors 1-deoxymannojirimycin and N-methyl-1-deoxynojirimycin in the rat *in vivo*. *Pharm. Res.*, **9**, 1442–1450 (1992).
14) Faber, E. D., Proost, J. H., Oosting, R., and Meijer, D. K., Disposition of glycosidase inhibitors in the isolated perfused rat liver: hepatobiliary and subcellular concentration gradients of 1-deoxymannojirimycin and N-methyl-1-deoxynojirimycin. *Pharm. Res.*, **11**, 144–150 (1994).
15) Treiber, A., Morand, O., and Clozel, M., The pharmacokinetics and tissue distribution of the glucosylceramide synthase inhibitor miglustat in the rat. *Xenobiotica*, **37**, 298–314 (2007).

Preparation of pure lipid hydroperoxides[S]

Daigo Ibusuki,* Kiyotaka Nakagawa,* Akira Asai,† Shinichi Oikawa,† Yuichi Masuda,* Toshihide Suzuki,§ and Teruo Miyazawa[1,*]

Food and Biodynamic Chemistry Laboratory,* Graduate School of Agricultural Science, Tohoku University, Sendai 981-8555, Japan; Department of Medicine,† Nippon Medical School, Tokyo 113-8602, Japan; and Faculty of Pharmaceutical Science,§ Teikyo University, Kanagawa 199-0195, Japan

Abstract **Increasing evidence of lipid peroxidation in food deterioration and pathophysiology of diseases have revealed the need for a pure lipid hydroperoxide (LOOH) reference as an authentic standard for quantification and as a compound for biological studies in this field. Generally, LOOH is prepared from photo- or enzymatically oxidized lipids; however, separating LOOH from other oxidation products and preparing pure LOOH is difficult. Early studies showed the usability of reaction between hydroperoxide and vinyl ether for preparation of pure LOOH. Because the reactivity of vinyl ether with LOOHs other than fatty acid hydroperoxides has never been reported, here, we employed the reaction for preparation of a wide variety of pure LOOHs. Phospholipid, cholesteryl ester, triacylglycerol, or fatty acid was photo- or enzymatically oxidized; the resultant crude sample containing hydroperoxide was allowed to react with a vinyl ether [2-methoxypropene (MxP)]. Liquid chromatography (LC) and mass spectrometry confirmed that MxP selectively reacts with LOOH, yielding a stable MxP adduct (perketal). The lipophilic perketal was eluted at a position away from that of intact LOOH and identified and isolated by LC. Upon treatment with acid, perketal released the original LOOH, which was finally purified by LC. Using our optimized purification procedures, for instance, we produced 75 mg of pure phosphatidylcholine hydroperoxide (>99%) from 100 mg of phosphatidylcholine. Our developed method expands the concept of the perketal method, which provides pure LOOH references. The LOOHs prepared by the perketal method would be used as "gold standards" in LOOH methodology.**—Ibusuki, D., K. Nakagawa, A. Asai, S. Oikawa, Y. Masuda, T. Suzuki, and T. Miyazawa. **Preparation of pure lipid hydroperoxides.** ***J. Lipid Res.*** **2008.** 49: **2668–2677.**

Supplementary key words oxidative stress • lipid peroxidation • lipid hydroperoxide standard • 2-methoxypropene

Because lipid peroxidation is involved in food deterioration (1) and pathophysiology of human diseases (2, 3), there has been a great interest in the accurate measurement of lipid hydroperoxide (LOOH) concentration. This can be performed by several quantitative methods (4–11), and the most sensitive and reliable one is chemiluminescence detection-liquid chromatography (CL-LC) (9–11). Since there is no approved LOOH calibrator ("gold standard") available, it is impossible to compare the LOOH levels from various laboratories around the world.

Currently, researchers prepare their own in-house reference LOOH [i.e., lipids (e.g., phospholipids, cholesterols, triacylglycerols, and fatty acids)] are subjected to photo- (12), free radical (13), or enzymatic oxidation (14, 15). The resultant crude or partly purified LOOH is generally used as a calibrator. However, these references are neither officially approved nor do they correspond to each other, particularly with regard to their purity. As frequently mentioned by LOOH researchers, this problem is mainly caused by the difficulty in distinguishing and isolating LOOH from other oxidation products such as hydroxides (13). Therefore, efficient purification of a wide variety of LOOHs is the key to the development of the gold standard not only for the accurate quantification of LOOH but also for the evaluation of its biological functions.

A few previous studies (16–21) have reported that some vinyl ether compounds [i.e., 2-methoxypropene (MxP)] react with organic hydroperoxides to yield perketals. These perketals, upon treatment with acid, release the original hydroperoxides. For instance, by using these reactions, Porter et al. (19) succeeded in purifying fatty acid methyl

This work was supported by KAKENHI (20228002) of JSPS, Japan.

Manuscript received 12 June 2008 and in revised form 27 June 2008.

Published, JLR Papers in Press, July 18, 2008.
DOI 10.1194/jlr.D800034-JLR200

Abbreviations: ChL, cholesteryl linoleate; CL, chemiluminescence; ESI, electrospray ionization; LA, linoleic acid; LAMe, methyl linoleate; LC, liquid chromatography; LLL, trilinoleoylglycerol; LOOH, lipid hydroperoxide; LOX-1, lipoxygenase-1; MS, mass spectrometry; MxP, 2-methoxypropene; PLPC, 1-palmitoyl-2-linoleoyl-*sn*-glycero-3-phosphocholine; PLPCOOH, 1-palmitoyl-2-hydroperoxyoctadecadienoyl-*sn*-glycero-3-phosphocholine; PLPCOOMxP, MxP adduct of PLPCOOH; PLPE, 1-palmitoyl-2-linoleoyl-*sn*-glycero-3-phosphoethanolamine; PLPS, 1-palmitoyl-2-linoleoyl-*sn*-glycero-3-phosphoserine; PPTS, pyridinium *p*-toluenesulfonate; RB, rose bengal; TIC, total ion chromatogram; Tris, tris(hydroxymethyl)aminomethane; UV, ultraviolet; XIC, extracted ion chromatogram.

[1] To whom correspondence should be addressed.
e-mail: miyazawa@biochem.tohoku.ac.jp

[S] The online version of this article (available at http://www.jlr.org) contains supplementary data in the form of six figures.

ester hydroperoxides. The reactivity of MxP with LOOHs other than fatty acid methyl ester hydroperoxides has never been reported; but these studies (16–21) indicated that the reaction may be useful for the preparation of a wide variety of pure LOOHs (**Fig. 1A**).

In the present study, we optimized the reaction between MxP and the hydroperoxides of phospholipids, cholesterol esters, triacylglycerols, fatty acids, and fatty acid methyl esters and developed a purification method of authentic LOOHs by photo- or enzymatic oxidation of lipids followed by derivatization with MxP and liquid chromatography (LC) isolation.

MATERIALS AND METHODS

Materials

We purchased 1-palmitoyl-2-linoleoyl-*sn*-glycero-3-phosphocholine (PLPC), trilinoleoylglycerol (LLL), linoleic acid (LA), methyl linoleate (LAMe), and pyridinium *p*-toluenesulfonate (PPTS) from Sigma (St. Louis, MO). We obtained 1-palmitoyl-2-linoleoyl-*sn*-glycero-3-phosphoethanolamine (PLPE) and 1-palmitoyl-2-linoleoyl-*sn*-glycero-3-phosphoserine (PLPS) from Avanti Polar Lipids (Alabaster, AL). Cholesteryl linoleate (ChL) was obtained from ICN Biomedicals Inc. (Aurora, OH). All other reagents were of analytical grade.

LOOH preparation

In order to prepare LOOH, the lipid (PLPC, PLPE, PLPS, ChL, LLL, LA, or LAMe; Fig. 1B) was subjected to three different types of oxidations [rose bengal (RB)-catalyzed photo-oxidation, ultraviolet (UV) photo-oxidation, and lipoxygenase-catalyzed oxidation].

For RB-catalyzed photo-oxidation, PLPC, PLPE, PLPS, LA, or LAMe (100 mg) was dissolved in 5 ml of methanol, whereas ChL or LLL (100 mg) was dissolved in 5 ml of chloroform/methanol (1:1, v/v). RB (CHROMA, Tokyo, Japan) was added to these samples at a concentration of 0.1 mg/ml. The samples were exposed to oxygen gas for 10 s and photo-oxidized for 3–24 h at 4°C (ice-cold conditions). A 100 W incandescent lamp (Matsushita Electric Industrial Co., Osaka, Japan) was positioned vertically 10 cm above the sample. Subsequently, to remove RB, the resultant sample of PLPC, PLPE, LAMe, ChL, or LLL was loaded onto a Sep-Pak Plus QMA column (Waters, Milford, MA). The column was eluted with 5 ml of methanol for PLPC, PLPE, and LAMe

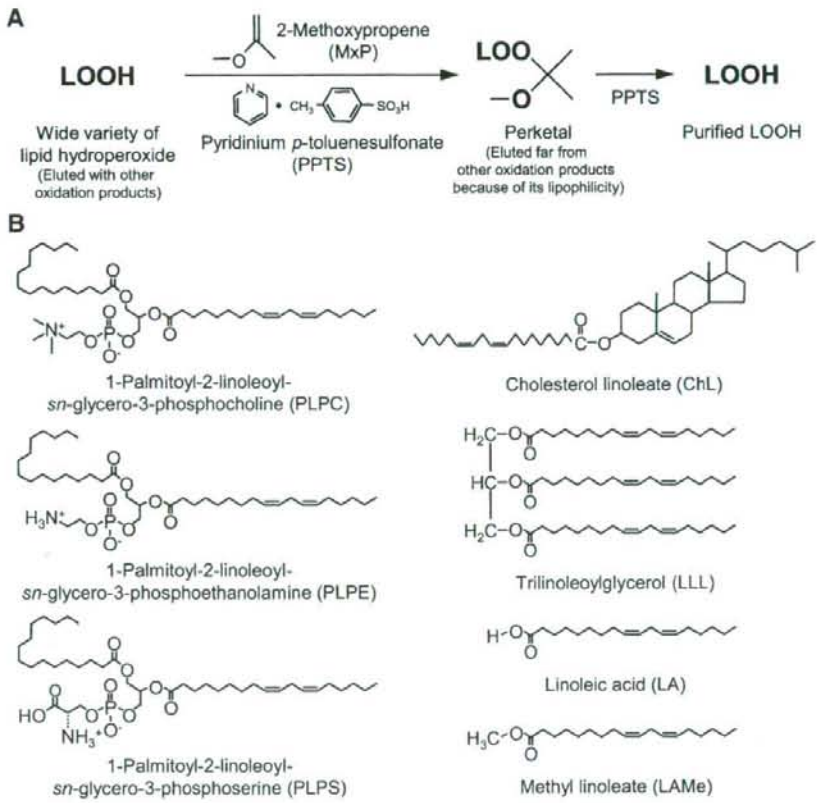

Fig. 1. A: Protocols investigated for the purification of lipid hydroperoxide (LOOH) using 2-methoxypropene (MxP). B: Chemical structures of lipids [1-palmitoyl-2-linoleoyl-*sn*-glycero-3-phosphocholine (PLPC), 1-palmitoyl-2-linoleoyl-*sn*-glycero-3-phosphoethanolamine (PLPE), 1-palmitoyl-2-linoleoyl-*sn*-glycero-3-phosphoserine (PLPS), cholesteryl linoleate (ChL), trilinoleoylglycerol (LLL), linoleic acid (LA), and methyl linoleate (LAMe)].

samples or with 5 ml of chloroform/methanol (1:1, v/v) for ChL and LLL samples. The eluent was collected, evaporated, and redissolved in 20 ml of dichloromethane. The PLPS and LA sample solutions were diluted with 5 ml of water and then loaded onto a flush column filled with 20 g of COSMOSIL $75C_{18}$-PREP ODS (Nacalai Tesque, Kyoto, Japan). The column was washed with 100 ml of methanol/water (1:1, v/v) to remove RB and eluted with 50 ml of methanol. The eluent was evaporated and redissolved in 20 ml of dichloromethane.

For UV photo-oxidation, 100 mg of PLPC, PLPE, PLPS, ChL, LLL, LA, or LAMe was placed in a test tube and exposed to oxygen gas for 10 s. The tube was capped, and then photo-oxidized using a 15 W UV GL-15 lamp (radiation frequency, 253 nm; Toshiba Electronics Co., Tokyo, Japan) at 20°C (room temperature) for 3–24 h. The light source was held vertically at 30 cm above the test tube. The resultant lipid was dissolved in 20 ml of dichloromethane.

For lipoxygenase-catalyzed oxidation, a solution of PLPC, PLPE, PLPS, LLL, LA, or LAMe (100 mg/5 ml of ethanol) was mixed with 170 ml of 50 mM borate buffer (pH 9.0) containing soybean lipoxygenase-1 (LOX-1, 1.25×10^6 units; SERVA Electrophoresis, Heidelberg, Germany) and sodium deoxycholate (375 mg). The mixture was incubated at 20–40°C for 3–24 h in the presence of oxygen. ChL (100 mg) was suspended in 5 ml of isopropanol and subjected to LOX-1-oxidation. The lipid moiety was then extracted by adding 30 ml of 0.2 M HCl and 60 ml of diethylether. After shaking the solution, the diethylether layer was collected, dried, and dissolved in 20 ml of dichloromethane.

A portion (1 μl) of the dichloromethane sample was subjected to LC combined with UV, chemiluminescence (CL), and mass spectrometry (MS) (LC-UV/CL/MS) (22, 23) to evaluate LOOH formation, as described below.

Purification of LOOH by using MxP

We confirmed LOOH formation in the dichloromethane sample allowed the sample to react with MxP in order to obtain perketal, and subsequently, LOOH was regenerated from the perketal as follows.

For the reaction with MxP, the dichloromethane sample (20 ml) was mixed with PPTS (2–10 mg/4 ml of dichloromethane). To the sample mixture, 1–5 g (approximately 1.3–6.7 ml) of MxP (Wako, Osaka, Japan) was added. The sample (total approximately 25–31 ml) was vortexed for 1 min and kept standing for 0.5–6 h at 4–20°C. After confirming the perketal formation by LC-UV/CL/MS, a portion (1 ml) of the sample mixture was subjected to semipreparative LC, and the perketal fraction was collected as described below. This isolation procedure was repeated 25–31 times. The collected perketal fractions were combined and evaporated to dryness.

For regeneration of LOOH, the isolated perketal was dissolved in 25 ml of chloroform/methanol (1:1, v/v). The solution was then mixed with PPTS [1–20 mg/5 ml of chloroform/methanol (1:1, v/v)] and incubated for 3–24 h at 4–37°C. After the regeneration of LOOH was ascertained by LC-UV/CL/MS, the LOOH was finally purified by semipreparative LC. The structure and purity of the obtained LOOH was evaluated by LC-UV/CL/MS. In addition, ^1H and ^{13}C nuclear magnetic resonance (NMR) spectra were recorded on a Varian Unity Plus-600 spectrometer (Palo Alto, CA) at 600 MHz for ^1H NMR and at 150 MHz for ^{13}C NMR using $CDCl_3$ as a solvent.

LC-UV/CL/MS for LOOH and perketal analysis

LOOH and its MxP adduct (perketal) were analyzed and their concentrations were determined by reversed-phase LC-UV/CL/MS. We used an ODS column (COSMOSIL $5C_{18}$-MS-II, 5 μm, 4.6 × 250 mm; Nacalai Tesque, Kyoto, Japan) fitted with its precolumn (4.6 × 10 mm). The column was eluted with methanol/water (100:5, v/v) containing 5 mM ammonium acetate for PLPC, PLPE, and PLPS samples; methanol/ethanol (100:30, v/v) for the ChL sample; methanol/ethanol (100:10, v/v) for the LLL sample; methanol/water (100:30, v/v) containing 0.1% acetic acid for the LA sample; and methanol/water (100:20, v/v) for the LAMe sample. The flow rate was adjusted to 1 ml/min and column temperature was maintained at 40°C. After the column eluent was monitored with a UV detector (UV-970; JASCO, Tokyo, Japan) at 210 nm, the eluent was divided into two portions. One portion (0.99 ml/min) was mixed with hydroperoxide-specific CL reagent (a mixture of cytochrome c and luminol in 50 mM borate buffer, pH 10.0) (10, 11) and introduced into a CL detector (825-CL;

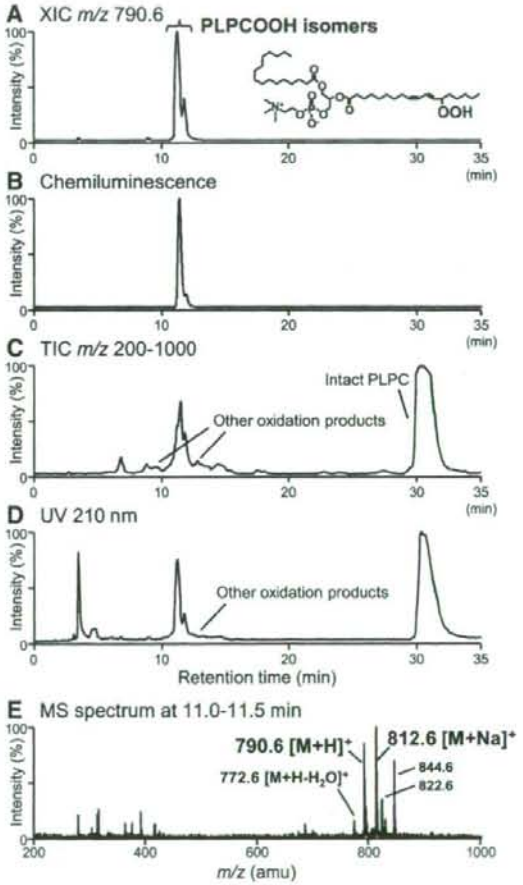

Fig. 2. Preparation of 1-palmitoyl-2-hydroperoxyoctadecadienoyl-*sn*-glycero-3-phosphocholine (PLPCOOH). PLPC [100 mg/5 ml of methanol, containing 0.5 mg of rose bengal (RB)] was photo-oxidized for 8 h at 4°C, and analyzed by liquid chromatography ultraviolet (LC-UV)/chemiluminescence (CL)/mass spectrometry (MS). A: Extracted ion chromatogram (XIC) of PLPCOOH (*m/z* 790.6 $[M+H]^+$) and its representative isomer [1-palmitoyl-2-(13-hydroperoxy-9*Z*,11*E*-octadecadienoyl)-*sn*-glycero-3-phosphocholine]. B: CL chromatogram. C: Total ion chromatogram (TIC, *m/z* 200–1000). D: UV chromatogram (at 210 nm). E: MS spectrum at 11.0–11.5 min.

JASCO). The flow rate of the CL reagent was set at 0.5 ml/min. The second portion (0.01 ml/min) was introduced into a Mariner electrospray ionization (ESI) time-of-flight mass spectrometer (Applied Biosystems, Foster City, CA). The MS parameters were positive-ion measurement mode (spray voltage, 3000 V; nozzle potential, 100 V; nozzle temperature, 140°C; flow rate of nebulizer gas, 0.75 l/min; and that of spray gas, 2.0 l/min), but were negative-ion mode for the PLPS sample. Full-scan mass spectra were recorded over a range of m/z 200–1300 in a scan time of 3 s.

Semipreparative LC for perketal and LOOH isolation

Perketal and LOOH (regenerated from perketal) were isolated using semipreparative LC by using an ODS column (COSMOSIL $5C_{18}$-MS-II, 5 μm, 20 × 250 mm; Nacalai Tesque) fitted with its precolumn (10 × 50 mm). The mobile phases used were the same as those used for LC-UV/CL/MS, as described above. The flow rate was 10 ml/min and column temperature was maintained at 40°C. After the column eluent was monitored with a UV detector at 210 and 234 nm, the fraction of perketal or LOOH was collected.

Structural determination of PLPCOOH isomers

1-Palmitoyl-2-hydroperoxyoctadecadienoyl-*sn*-glycero-3-phosphocholine (PLPCOOH, about 0.8 mg), purified from RB-photo-oxidation or LOX-1 oxidation sample, was dissolved in 1 ml of methanol. To the solution, 2 mg of sodium borohydride ($NaBH_4$) was added and mixed for 30 min at room temperature. To the reaction mixture, 0.1 ml of 4 M HCl, 2 ml of chloroform and 1 ml of water were added to remove remaining $NaBH_4$ (24).

TABLE 1. Optimal oxidation procedure to prepare LOOH

Lipid		Oxidation procedure	Time	Temp	Yielded LOOH[a]	
	mg		*h*	*°C*		*mg*
PLPC	100	RB-photo	8	4	PLPCOOH	30
	100	UV-photo	24	20	PLPCOOH	1.7
	100	LOX-1	12	40	PLPCOOH	96
PLPE	100	RB-photo	10	4	PLPEOOH	28
	100	UV-photo	24	20	PLPEOOH	1.4
	100	LOX-1	12	40	PLPEOOH	92
PLPS	100	RB-photo	10	4	PLPSOOH	30
	100	UV-photo	24	20	PLPSOOH	1.3
	100	LOX-1	12	40	PLPSOOH	94
ChL	100	RB-photo	8	4	ChLOOH	27
	100	UV-photo	24	20	ChLOOH	1.1
	100	LOX-1	24	40	ChLOOH	6.2
LLL	100	RB-photo	6	4	LLLOOH	31
	100	UV-photo	6	20	LLLOOH	35
	100	LOX-1	12	40	LLLOOH	9.4
LA	100	RB-photo	8	4	LAOOH	32
	100	UV-photo	12	20	LAOOH	35
	100	LOX-1	6	20	LAOOH	99
LAMe	100	RB-photo	8	4	LAMeOOH	34
	100	UV-photo	12	20	LAMeOOH	36
	100	LOX-1	8	20	LAMeOOH	97

LOOH, lipid hydroperoxide; LOX-1, lipoxygenase-1; PLPC, 1-palmitoyl-2-linoleoyl-*sn*-glycero-3-phosphocholine; PLPCOOH, 1-palmitoyl-2-hydroperoxyoctadecadienoyl-*sn*-glycero-3-phosphocholine; PLPE, 1-palmitoyl-2-linoleoyl-*sn*-glycero-3-phosphoethanolamine; RB, rose bengal; UV, ultraviolet.

[a] LC retention times and mass spectrometry (MS) profiles of hydroperoxides are as follows; PLPCOOH, 11.0 min, 790.6 $[M+H]^+$; PLPEOOH, 10.5 min, 748.5 $[M+H]^+$; PLPSOOH, 8.5 min, 790.4 $[M-H]^-$; ChLOOH, 26.5 min, 703.6 $[M+Na]^+$; LLLOOH, 23.0 min, 933.7 $[M+Na]^+$; LAOOH, 15.5 min, 330.3 $[M+NH_4]^+$; LAMeOOH, 11.5 min, 349.3 $[M+Na]^+$.

After centrifugation at 1000 *g* for 5 min at 4°C, the lower chloroform layer was collected and dried under N_2 gas. The dried extract was dissolved in 1 ml of methanol, mixed with 1 ml of 50 mM HCl-Tris [tris(hydroxymethyl)aminomethane] buffer (pH 7.4, containing 1 mg of calcium chloride and 1,500 units of phosphaolipase A_2 (from honey bee venom; Sigma, St. Louis, MO), and incubated for 2 h at room temperature (25). After centrifugation at 1,000 *g* for 5 min at 4°C, the lower chloroform layer was collected and dried by N_2 gas. The dried residue was redissolved in 1 ml of methanol, and subjected to semipreparative LC for isolation of hydroxy-LA. An ODS column (COSMOSIL $5C_{18}$-MS-II, 5 μm, 20 × 250 mm; Nacalai Tesque, Kyoto, Japan) was eluted with a mixture of methanol/water (100:25, v/v). The flow rate

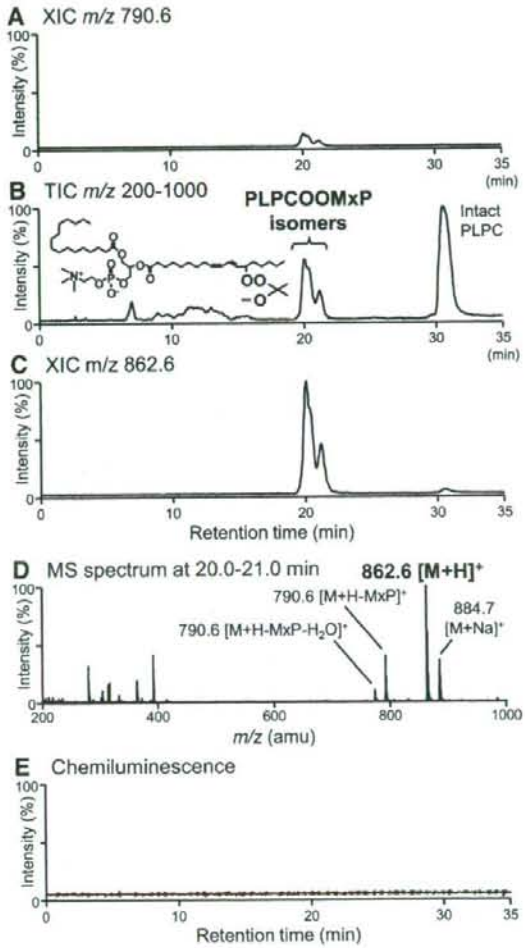

Fig. 3. Conversion of PLPCOOH to MxP adduct of PLPCOOH (PLPCOOMxP) (perketal). RB-catalyzed photo-oxidized PLPC sample (20 ml) was mixed with pyridinium *p*-toluenesulfonate (PPTS) (5 mg/4 ml of dichloromethane) and 3 g (4 ml) of MxP. The sample was maintained for 3 h at 4°C, and then analyzed by LC-UV/CL/MS. A: XIC of PLPCOOH (m/z 790.6 $[M+H]^+$). B: TIC (m/z 200–1000) and structure of PLPCOOMxP (representative MxP adduct of PLPCOOH isomer in Fig. 2). C: XIC of PLPCOOMxP (m/z 862.6 $[M+H]^+$). D: MS spectrum at 20.0–21.0 min. E: CL chromatogram.

TABLE 2. Optimal MxP reaction condition to prepare perketal

Sample	in 20 ml of dichloromethane			Added PPTS mg/4 ml of dichloromethane	Added MxP g	Added MxP (ml)	Total reaction volume ml	Time h	Temp °C	Yielded perketal[c]		Perketal after LC isolation mg
PLPC	(RB-photo,[a]	30	mg PLPCOOH[b])	5	3	(4.0)	28	3	4	PLPCOOMxP	30	28
	(UV-photo,	1.7	mg PLPCOOH)	2	1	(1.3)	25	2	4	PLPCOOMxP	1.6	1.5
	(LOX-1,	96	mg PLPCOOH)	5	3	(4.0)	28	3	4	PLPCOOMxP	96	92
PLPE	(RB-photo,	28	mg PLPEOOH)	5	3	(4.0)	28	3	4	PLPEOOMxP	27	22
	(UV-photo,	1.4	mg PLPEOOH)	2	1	(1.3)	25	2	4	PLPEOOMxP	1.3	1.0
	(LOX-1,	92	mg PLPEOOH)	5	3	(4.0)	28	3	4	PLPEOOMxP	90	86
PLPS	(RB-photo,	30	mg PLPSOOH)	5	3	(4.0)	28	3	4	PLPSOOMxP	27	24
	(UV-photo,	1.3	mg PLPSOOH)	2	1	(1.3)	25	2	4	PLPSOOMxP	1.2	1.0
	(LOX-1,	94	mg PLPSOOH)	5	3	(4.0)	28	3	4	PLPSOOMxP	88	83
ChL	(RB-photo,	27	mg ChLOOH)	5	5	(6.7)	31	3	20	ChLOOMxP	26	20
	(UV-photo,	1.1	mg ChLOOH)	2	2	(2.7)	27	3	20	ChLOOMxP	1.0	0.9
	(LOX-1,	6.2	mg ChLOOH)	2	2	(2.7)	27	3	20	ChLOOMxP	5.9	5.3
LLL	(RB-photo,	31	mg LLLOOH)	10	5	(6.7)	31	3	20	LLLOOMxP	30	27
	(UV-photo,	35	mg LLLOOH)	10	5	(6.7)	31	3	20	LLLOOMxP	33	32
	(LOX-1,	9.4	mg LLLOOH)	5	3	(4.0)	28	3	20	LLLOOMxP	9.3	8.2
LA	(RB-photo,	32	mg LAOOH)	2	1	(1.3)	25	1	4	LAOOMxP	30	24
	(UV-photo,	35	mg LAOOH)	2	1	(1.3)	25	1	4	LAOOMxP	32	26
	(LOX-1,	99	mg LAOOH)	5	2	(2.7)	27	1	4	LAOOMxP	95	85
LAMe	(RB-photo,	34	mg LAMeOOH)	2	1	(1.3)	25	1	4	LAMeOOMxP	34	30
	(UV-photo,	36	mg LAMeOOH)	2	1	(1.3)	25	1	4	LAMeOOMxP	36	33
	(LOX-1,	97	mg LAMeOOH)	5	2	(2.7)	27	1	4	LAMeOOMxP	97	93

[a] Oxidation procedure.
[b] LOOH concentration in sample.
[c] LC retention times and MS profiles of perketals are as follows: PLPCOOMxP, 20.0 min, 862.6 $[M+H]^+$; PLPEOOMxP, 18.5 min, 820.6 $[M+NH_4]^+$; PLPSOOMxP, 15.5 min, 862.5 $[M-H]^-$; ChLOOMxP, 51.5 min, 775.6 $[M+Na]^+$; LLLOOMxP, 45.0 min, 1005.8 $[M+Na]^+$; LAOOMxP, 49.5 min, 402.3 $[M+NH_4]^+$; LAMeOOMxP, 33.5 min, 416.3 $[M+NH_4]^+$.

was 10 ml/min and the column temperature was at 40°C. The isolated hydroxy-LA was dried, dissolved in 1 ml of hexane (containing 4 μmol trimethylsilyl diazomethane), vortexed, and stored for 1 h at room temperature (26, 27). To the solution, 0.1 g of acetic acid and 1 ml of water were added to terminate the reaction. After that, the upper hexane layer (hydroxy-LAMe fraction) was analyzed by normal phase LC with a silica column (CAPCELL PAK SILICA SG120, 5 μm, 4.6 × 250 mm; Shiseido, Tokyo, Japan). A mixture of hexane/diethylether/water (87:13:0.1, v/v/v) was used as eluent at the flow rate of 1 ml/min. The column temperature was at 40°C. Hydroxy-LAMe isomers were detected by UV detector at 234 nm, and identified by their retention times (based on Refs. 28,29).

Stability testing

The obtained hydroperoxides of PLPC, PLPE, PLPS, LA, and LAMe (1.5 mg) were dissolved in 1 ml of methanol, while the hydroperoxides of ChL and LLL (1.5 mg) were dissolved in 1 ml of chloroform/methanol (1:1, v/v). These solutions were stored under nitrogen atmosphere at −30°C for 12 months and analyzed by LC-UV/CL/MS. Similarly, the stability of perketals was evaluated.

Statistics

The data are expressed as mean ± SD and analyzed using Student's *t*-test. Differences were considered significant at $P < 0.05$.

RESULTS

LOOH formation during photo- and enzymatic oxidation

We initially analyzed the RB-catalyzed photo-oxidation of PLPC (12). After the reaction, PLPCOOH (*m/z* 790.6 $[M+H]^+$) was formed as the major oxidation product (**Fig. 2A**) and also confirmed by CL detection (Fig. 2B). The PLPCOOH possessed four structural isomers of hydroperoxyoctadecadienoyl residues: 13-hydroperoxy-9*Z*,11*E*-octadecadienoate (retention time, 11.0 min), 9-hydroperoxy-10*E*,12*Z*-octadecadienoate (11.0 min), 13-hydroperoxy-9*E*,11*E*-octadecadienoate (11.5 min), and 9-hydroperoxy-10*E*,12*E*-octadecadienoate (11.5 min). Similarly, LOOH formation was verified when PLPC, PLPE, PLPS, ChL, LLL, LA, and LAMe were subjected to RB-catalyzed photo-, UV photo-, and LOX-1-catalyzed oxidation. Optimal conditions required for the maximum yield of LOOH are summarized in **Table 1**.

In the case of all samples, LOOH was coeluted with other oxidation products, particularly in photo-oxidation (as shown in the total ion chromatogram, UV chromatogram, and MS spectrum of PLPCOOH, Figs. 2C–E). This fact indicates that distinguishing and separating LOOH from other hydroperoxides is difficult.

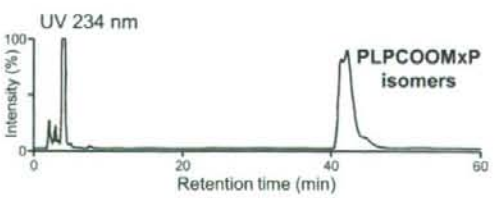

Fig. 4. PLPCOOMxP isolation. PLPCOOMxP sample obtained in Fig. 3 was isolated by semipreparative LC monitored by UV absorption at 234 nm.

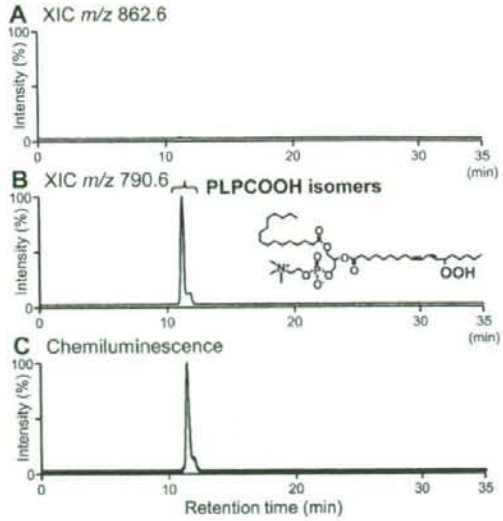

Fig. 5. PLPCOOH regeneration. PLPCOOMxP isolated in Fig. 4 (25 ml) was mixed with PPTS [10 mg/5 ml of chloroform/methanol (1:1)], maintained for 6 h at 4°C, and the sample was then analyzed by LC-UV/CL/MS. A: XIC of PLPCOOMxP (m/z 862.6 $[M+H]^+$). B: XIC of PLPCOOH (m/z 790.6 $[M+H]^+$) and its representative isomer (regenerated PLPCOOMxP isomer). C: CL chromatogram.

Reaction of LOOH with MxP

The photo- and enzymatically oxidized lipid samples were treated with MxP. After treating the RB-catalyzed photo-oxidized PLPC sample with MxP, PLPCOOH isomers were no longer detectable in the sample (**Fig. 3A**). Moreover, perketals (PLPCOOMxP isomers, m/z 862.6 $[M+H]^+$) were detected at around 20.0 min (Figs. 3B–D). These isomers were CL-negative (Fig. 3E), indicating the absence of a hydroperoxide group.

In the case of other samples, MxP also reacted almost completely with LOOH to yield perketals. The optimal conditions required to obtain perketals with good efficiency are described in **Table 2**. Due to the lipophilic nature of perketal, it was eluted at a position away from that of the intact LOOH, and therefore easily isolated by semipreparative LC (refer to the isolation of PLPCOOMxP peak in **Fig. 4**).

Regeneration of intact LOOH from perketal

To regenerate LOOH, each isolated perketal was treated with acid (i.e., PPTS). For example, after treatment of the PLPCOOMxP with PPTS, they were no longer detectable, and PLPCOOH isomers were regenerated as compounds corresponding to clear peaks in MS and CL chromatograms (**Fig. 5**). Other perketals were also efficiently converted to original hydroperoxides under optimized conditions (**Table 3**).

Final purification of LOOH

Finally, the regenerated LOOH was purified by semipreparative LC. An example (isolation of PLPCOOH peak) is shown in **Fig. 6**. The obtained PLPCOOH was a pure mixture of isomers, as judged from the LC-UV/CL/MS data (**Fig. 7**) and NMR spectra (data not shown). The composition of hydroperoxyoctadecadienoyl residues of the obtained PLPCOOH was 13-hydroperoxy-9*Z*,11*E*-octadecadienoate

TABLE 3. Optimal LOOH regeneration condition from perketal

Isolated perketal		Added PPTS	Total reaction volume	Time	Temp	Yielded LOOH[b]		LOOH after LC isolation	Purity of isolated LOOH
in 25 ml of chloroform/methanol (1:1)		*mg/5 ml of chloroform/methanol (1:1)*	*ml*	*h*	*°C*		*mg*	*mg*	%
PLPCOOMxP	(RB-photo,[a] 28 mg)	10	30	6	4	PLPCOOH	27	16	98
	(UV-photo, 1.5 mg)	10	30	2	4	PLPCOOH	1.4	0.9	95
	(LOX-1, 92 mg)	10	30	12	4	PLPCOOH	90	75	>99
PLPEOOMxP	(RB-photo, 22 mg)	10	30	6	4	PLPEOOH	20	12	98
	(UV-photo, 1.0 mg)	10	30	2	4	PLPEOOH	0.9	0.6	94
	(LOX-1, 86 mg)	10	30	12	4	PLPEOOH	80	65	98
PLPSOOMxP	(RB-photo, 24 mg)	10	30	6	4	PLPSOOH	22	14	98
	(UV-photo, 1.0 mg)	10	30	2	4	PLPSOOH	0.9	0.6	93
	(LOX-1, 83 mg)	10	30	12	4	PLPSOOH	78	60	98
ChLOOMxP	(RB-photo, 20 mg)	10	30	6	20	ChLOOH	18	11	98
	(UV-photo, 0.9 mg)	10	30	2	20	ChLOOH	0.8	0.5	95
	(LOX-1, 5.3 mg)	10	30	2	20	ChLOOH	4.8	2.3	95
LLLOOMxP	(RB-photo, 27 mg)	10	30	6	4	LLLOOH	26	19	95
	(UV-photo, 32 mg)	10	30	6	4	LLLOOH	30	21	98
	(LOX-1, 8.2 mg)	10	30	6	4	LLLOOH	7.6	5.0	98
LAOOMxP	(RB-photo, 24 mg)	5	30	1	4	LAOOH	22	14	95
	(UV-photo, 26 mg)	5	30	1	4	LAOOH	24	16	95
	(LOX-1, 85 mg)	5	30	6	4	LAOOH	81	57	98
LAMeOOMxP	(RB-photo, 30 mg)	5	30	1	4	LAMeOOH	28	19	95
	(UV-photo, 33 mg)	5	30	1	4	LAMeOOH	31	20	97
	(LOX-1, 93 mg)	5	30	6	4	LAMeOOH	90	78	>99

[a] Oxidation procedure.

[b] LC retention times and MS profiles of hydroperoxides are as follows; PLPCOOH, 11.0 min, 790.6 $[M+H]^+$; PLPEOOH, 10.5 min, 748.5 $[M+H]^+$; PLPSOOH, 8.5 min, 790.4 $[M-H]^-$; ChLOOH, 26.5 min, 703.6 $[M+Na]^+$; LLLOOH, 23.0 min, 933.7 $[M+Na]^+$; LAOOH, 15.5 min, 330.3 $[M+NH_4]^+$; LAMeOOH, 11.5 min, 349.3 $[M+Na]^+$.

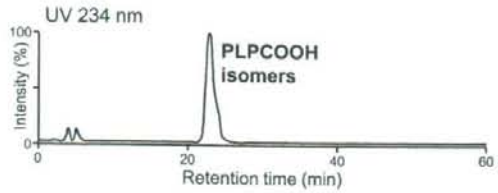

Fig. 6. PLPCOOH isolation. PLPCOOMxP sample regenerated in Fig. 5 was isolated by semipreparative LC monitored by UV absorption at 234 nm.

(46%), 9-hydroperoxy-10*E*,12*Z*-octadecadienoate (43%), 13-hydroperoxy-9*E*,11*E*-octadecadienoate (7%), and 9-hydroperoxy-10*E*,12*E*-octadecadienoate (4%). For other hydroperoxides of PLPE, PLPS, ChL, LLL, LA, and LAMe, pure mixtures of hydroperoxide isomers could also be prepared (see supplementary Figs. I–VI).

On the other hand, when LOX-1-catalyzed oxidation was conducted instead of photo-oxidation, we obtained an LOOH isomer (e.g., PLPCOOH bearing 13-hydroperoxy-9*Z*,11*E*-octadecadienoate) with high purity and yield.

Stability of LOOHs and perketals

About 9% of PLPCOOH was decomposed after 12 months during storage at −30°C (**Fig. 8**). In contrast, PLPCOOMxP (perketal) was more stable (about 97% remained) than PLPCOOH. The stabilities (measured as % wt remaining) of other hydroperoxides and perketals at 12 months after preparation were as follows: PLPEOOH (63%), PLPEOOMxP (91%); PLPSOOH (50%), PLPSOOMxP (85%); ChLOOH (89%), ChLOOMxP (94%); LLLOOH (86%), LLLOOMxP (95%); LAOOH (40%), LAOOMxP (78%); and LAMeOOH (90%), LAMeOOMxP (98%).

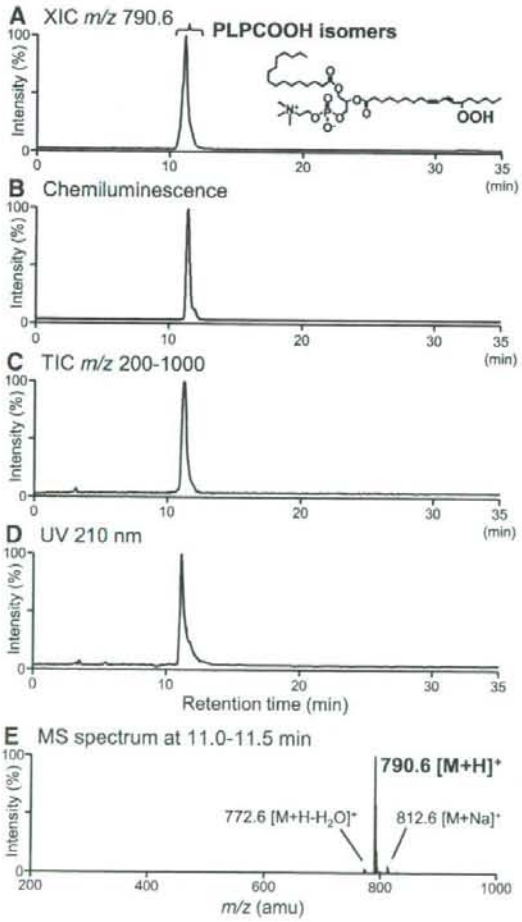

Fig. 7. Purity determination of PLPCOOH. PLPCOOH prepared by the final isolation in Fig. 6 was analyzed by LC-UV/CL/MS. A: XIC of PLPCOOH (m/z 790.6 $[M+H]^+$) and its representative isomer. B: CL chromatogram. C: TIC (m/z 200–1000). D: UV chromatogram (absorbance at 210 nm). E: MS spectrum at 11.0–11.5 min.

DISCUSSION

The oxidative modification of lipids, particularly LOOH accumulation, plays a major role in food deterioration (1) and pathophysiology of human diseases, such as atherogenesis, diabetes, and dementia, and aging (2, 3, 30–34). Accurate measurement of LOOH levels is therefore important, but no approved LOOH standard is available yet. In this study, we developed a method for the preparation of the hydroperoxides of PLPC, PLPE, PLPS, ChL, LLL, LA, and LAMe through reaction with MxP.

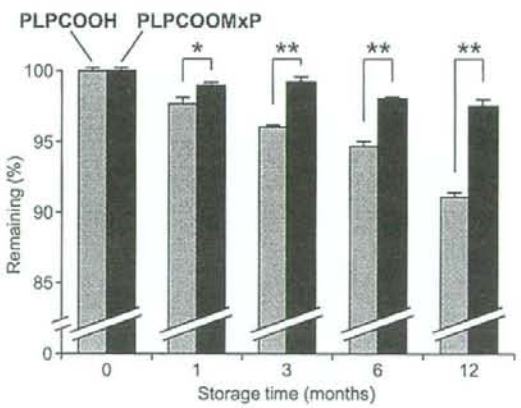

Fig. 8. Stabilities of PLPCOOH and PLPCOOMxP. PLPCOOH in Fig. 6 and PLPCOOMxP in Fig. 4 (1.5 mg/1 ml of methanol) were stored under nitrogen atmosphere at −30°C for approximately 12 months, and the remaining were analyzed by XIC of PLPCOOH (m/z 790.6 $[M+H]^+$) or XIC of PLPCOOMxP (m/z 862.6 $[M+H]^+$) on LC-UV/CL/MS compared with XIC (m/z 758.6 $[M+H]^+$) of PLPC reference. The data are expressed as mean ± SD, n = 3, and analyzed using Student's *t*-test. Differences were considered significant at * $P < 0.05$ or ** $P < 0.01$.

Over 50 years ago, it was reported that under acidic conditions, some vinyl ethers can react with organic hydroperoxides to form perketals (16, 17). At around 1990, Porter et al. (18, 19) reported the application of vinyl ether (*trans*-2-phenylcyclohexyl 2-propen-2-yl ether) for the synthesis of optically pure hydroperoxides (e.g., α-phenethyl hydroperoxide, 2-octyl hydroperoxide, and some fatty acid methyl ester hydroperoxides). The procedures include protecting the racemic hydroperoxides as perketals by using vinyl ether, separating the perketal diastereomers by chromatography, and regenerating the optically pure hydroperoxides from the perketal diastereomers. Baba et al. (21) used MxP for the conversion of LAMeOOH into its perketal. The perketal was utilized for preparation of PLPCOOH (21), but the preparation needed several synthetic steps. In this study, we thought that if MxP reacts efficiently with a variety of LOOHs (refer to the beginning of this article), this reaction can be applied for preparation of pure LOOHs (Fig. 1A).

We investigated and optimized the preparation conditions of LOOH (Fig. 2 and Table 1). Under optimal conditions, when the lipid used (PLPC, PLPE, PLPS, ChL, LLL, LA, or LAMe) was subjected to RB-catalyzed photo-, UV photo-, or LOX-1-catalyzed oxidation, the unsaturated fatty acid (linoleoyl) residue was converted to hydroperoxides. In cases of RB-catalyzed photo- and UV photo-oxidation of lipids, the structure of hydroperoxy linoleic residue was characterized as a mixture of 13-hydroperoxy-9*Z*,11*E*-octadecadienoate, 9-hydroperoxy-10*E*,12*Z*-octadecadienoate, 13-hydroperoxy-9*E*,11*E*-octadecadienoate, and 9-hydroperoxy-10*E*,12*E*-octadecadienoate. In LOX-1-catalyzed oxidation, 13-hydroperoxy-9*Z*,11*E*-octadecadienoate was produced predominantly. In addition, we found that RB-catalyzed photo- and UV photo-oxidation of ChL yielded mono-hydroperoxide as well as bis-hydroperoxide. Moreover, these reactions produced mono-, bis-, and tris-hydroperoxides of LLL. These LOOHs were partly decomposed to a wide range of secondary oxidation products, including hydroxides, epoxides, aldehydes, and ketones. These secondary oxidation products were the major obstacle in the isolation of pure LOOH.

For the reaction of LOOH with MxP, one of the important parameters was the reaction solvent. We found that dichloromethane, chloroform, or acetonitrile could be used as a solvent, but other water-containing solvents inhibited the reaction. Reaction temperature is also important since high temperatures (above 30°C) caused the formation of unknown products. Based on these results, we optimized the reaction conditions (Fig. 3 and Table 2). Under optimal conditions, LOOH was almost completely converted (above 90%) to perketal within a short time period of less than 3 h. The lipophilic perketal was eluted in a position apart from that of intact LOOH, and thereby the perketal could be identified and isolated by semipreparative LC (Fig. 4). No decomposition products of perketal were detected, indicating the stability of perketal. In addition, because MxP did not react with the secondary oxidation products, the isolation of perketal could be performed effectively. To reveal this point, we selected RB-photo-oxidized PLPC as an example (the example has an advantage to show that MxP reacts selectively to LOOHs but not to other oxidation secondary products derived from the RB-photo-oxidation).

A possible reaction scheme for the regeneration of intact LOOH from perketal is shown in **Fig. 9**. As shown in the scheme, the kind and the concentration of the acid used were important, and these factors were optimized (Fig. 5 and Table 3). In this study, chloroform/methanol (1:1, v/v) was used as the reaction solvent, and methanol or acetonitrile could also be used. Under optimal conditions, perketal

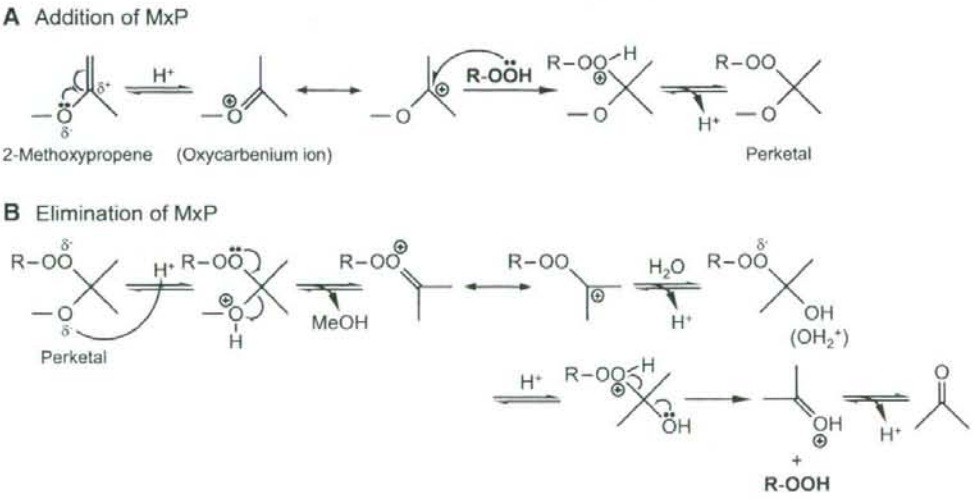

Fig. 9. Presumed mechanism of the reaction between MxP and hydroperoxide. A: Addition of MxP by nucleophilic addition of hydroperoxide to 2-methoxypropene. B: Elimination of MxP and regeneration of hydroperoxide.

was converted to original LOOH with a high yield (above 90%), and the regenerated LOOH was next subjected to final semipreparative LC purification (Fig. 6).

The obtained LOOHs after photo-oxidation were highly pure (Fig. 7, Table 3), but structural isomers were present (e.g., the prepared PLPCOOH contained mainly 13-hydroperoxy-9*Z*,11*E*-octadecadienoate and 9-hydroperoxy-10*E*,12*Z*-octadecadienoate). However, the "structural mixture" would be sufficient for use as a standard in most analytical and quantitative experiments. In contrast, when LOX-1-catalyzed oxidation was carried out, a pure LOOH isomer bearing 13-hydroperoxy-9*Z*,11*E*-octadecadienoate moiety was obtained. On the other hand, by using the present method, we prepared pure bis-hydroperoxide of ChL. Its structure was speculated based on the following findings: *1*) it reacted with two MxP molecules; and *2*) when the MxP adduct was subjected to alkaline hydrolysis, the reaction yielded LAOOMxP and perketal of cholesterol hydroperoxide.

With regard to the stability test, perketals were found to be more stable than LOOHs. Although perketal bearing an acidic carboxyl group (PLPSOOMxP or LAOOMxP) tended to degrade to some extent after 12 months storage at −30°C, such degradation was kept to a minimum by storage at −80°C for 3 months. We therefore recommended the following procedures: researchers should prepare and store perketals at −80°C in advance, regenerate LOOH from perketals before the experiment (e.g., quantitative study), and use the pure LOOH as the reference material.

In conclusion, we developed a convenient method for preparing a wide variety of pure LOOH references. We are now synthesizing and using the pure LOOH (e.g., PLPCOOH) as the standard for quantification of phosphatidylcholine hydroperoxide present in the blood plasma of healthy and nonhealthy humans, as well as a model compound to evaluate its biological functions in cell culture studies. We propose to use the MxP procedures developed by us as gold standard in the preparation method for the LOOH assay.

We thank Prof. Mari Yotsu-Yamashita and Dr. Yoshihiro Suzuki (Graduate School of Agricultural Science, Tohoku University) for help in NMR analysis, Associate Professor Masato Oikawa (Graduate School of Life Sciences, Tohoku University) for helpful discussions about reaction mechanism of LOOH with MxP, and Mr. Phumon Sookwong (Graduate School of Agricultural Science, Tohoku University) for excellent technical advice.

REFERENCES

1. Miyazawa, T., H. Kunika, K. Fujimoto, Y. Endo, and T. Kaneda. 1995. Chemiluminescence detection of mono-, bis-, and tris-hydroperoxy triacylglycerols present in vegetable oils. *Lipids.* **30:** 1001–1006.
2. Steinberg, D., S. Parthasarathy, T. E. Carew, J. C. Khoo, and J. L. Witztum. 1989. Beyond cholesterol. Modifications of low-density lipoprotein that increase its atherogenicity. *N. Engl. J. Med.* **320:** 915–924.
3. Stocker, R., and J. F. Keaney, Jr. 2004. Role of oxidative modifications in atherosclerosis. *Physiol. Rev.* **84:** 1381–1478.
4. Ohkawa, H., N. Ohishi, and K. Yagi. 1979. Assay for lipid peroxides in animal tissues by thiobarbituric acid reaction. *Anal. Biochem.* **95:** 351–358.
5. Marshall, P. J., M. A. Warso, and W. E. M. Lands. 1985. Selective microdetermination of lipid hydroperoxides. *Anal. Biochem.* **145:** 192–199.
6. Meguro, H., K. Akasaka, and H. Ohrui. 1990. Determination of hydroperoxides with fluorometric reagent diphenyl-1-pyrenylphosphine. *Methods Enzymol.* **186:** 157–161.
7. Cramer, G. L., J. F. Miller, Jr., R. B. Pendleton, and W. E. M. Lands. 1991. Iodometric measurement of lipid hydroperoxides in human plasma. *Anal. Biochem.* **193:** 204–211.
8. Jiang, Z. Y., J. V. Hunt, and S. P. Wolff. 1992. Ferrous ion oxidation in the presence of xylenol orange for detection of lipid hydroperoxide in low density lipoprotein. *Anal. Biochem.* **202:** 384–389.
9. Miyazawa, T. 1989. Determination of phospholipid hydroperoxides in human blood plasma by a chemiluminescence-HPLC assay. *Free Radic. Biol. Med.* **7:** 209–217.
10. Miyazawa, T., T. Suzuki, K. Fujimoto, and K. Yasuda. 1992. Chemiluminescent simultaneous determination of phosphatidylcholine hydroperoxide and phosphatidylethanolamine hydroperoxide in the liver and brain of the rat. *J. Lipid Res.* **33:** 1051–1059.
11. Miyazawa, T., K. Fujimoto, T. Suzuki, and K. Yasuda. 1994. Determination of phospholipid hydroperoxides using luminol chemiluminescence-high-performance liquid chromatography. *Methods Enzymol.* **233:** 324–332.
12. Nakajima, A., and H. Hidaka. 1993. Photosensitized oxidation of oleic acid, methyl oleate, and olive oil using visible light. *J. Photoch. Photobio. A.* **74:** 189–194.
13. Porter, N. A., R. A. Wolf, and H. Weenen. 1980. The free radical oxidation of polyunsaturated lecithins. *Lipids.* **15:** 163–167.
14. Funk, M. O., R. Isaac, and N. A. Porter. 1976. Preparation and purification of lipid hydroperoxides from arachidonic and gamma-linolenic acids. *Lipids.* **11:** 113–117.
15. Therond, P., M. Couturier, J. F. Demelier, and F. Lemonnier. 1993. Simultaneous determination of the main molecular species of soybean phosphatidylcholine or phosphatidylethanolamine and their corresponding hydroperoxides obtained by lipoxygenase treatment. *Lipids.* **28:** 245–249.
16. Rigaudy, J., and G. Izoret. 1953. Addition of hydroperoxides to activated double bonds of vinyl ethers. *Compt. Rend.* **236:** 2086–2088.
17. Schmitz, E., A. Rieche, and E. Beyer. 1961. Peroxyde aus ketenacetalen. *Chem. Ber.* **94:** 2921–2931.
18. Dussault, P., and N. A. Porter. 1988. The resolution of racemic hydroperoxides: the preparation of optically pure hydroperoxide natural products. *J. Am. Chem. Soc.* **110:** 6276–6277.
19. Porter, N. A., P. Dussault, R. A. Breyer, J. Kaplan, and J. Morelli. 1990. The resolution of racemic hydroperoxides: a chromatography-based separation of perketals derived from arachidonic, linoleic, and oleic acid hydroperoxides. *Chem. Res. Toxicol.* **3:** 236–243.
20. Dussault, P. H., and A. Sahli. 1990. An olefination-based route to unsaturated hydroperoxides. *Tetrahedron Lett.* **31:** 5117–5120.
21. Baba, N., K. Yoneda, S. Tahara, J. Iwasa, T. Kaneko, and M. Matsuo. 1990. A regioselective, stereoselective synthesis of a diacylglycerophosphocholine hydroperoxide by use of lipoxygenase and lipase. *J. Chem. Soc. Chem. Commun.* **18:** 1281–1282.
22. Tagiri-Endo, M., K. Ono, K. Nakagawa, M. Yotsu-Yamashita, and T. Miyazawa. 2002. Ozonation of PC in ethanol: separation and identification of a novel ethoxyhydroperoxide. *Lipids.* **37:** 1007–1012.
23. Tagiri-Endo, M., K. Nakagawa, T. Sugawara, K. Ono, and T. Miyazawa. 2004. Ozonation of cholesterol in the presence of ethanol: identification of a cytotoxic ethoxyhydroperoxide molecule. *Lipids.* **39:** 259–264.
24. Kambayashi, Y., Y. Yamamoto, and M. Nakano. 1998. Preferential hydrolysis of oxidized phosphatidylcholine in cholesterol-containing phosphatidylcholine liposome by phospholipase A2. *Biochem. Biophys. Res. Commun.* **245:** 705–708.
25. Müller, K. D., H. Husmann, H. P. Nalik, and G. Schomburg. 1990. Transesterification of fatty acids from microorganisms and human blood serum by trimethylsulfonium hydroxide (TMSH) for GC analysis. *Chromatographia.* **30:** 245–248.
26. Turnipseed, S. B., A. J. Allentoff, and J. A. Thompson. 1993. Analysis of trimethylsilylperoxy derivatives of thermally labile hydroperoxides by gas chromatography-mass spectrometry. *Anal. Biochem.* **213:** 218–225.
27. Mlakar, A., and G. Spiteller. 1996. Distinction between enzymic and nonenzymic lipid peroxidation. *J. Chromatogr. A.* **743:** 293–300.
28. Wang, X. H., T. Ohshima, H. Ushio, and C. Koizumi. 1999. Proportion of geometrical hydroperoxide isomers generated by radical oxidation of methyl linoleate in homogeneous solution and in aqueous emulsion. *Lipids.* **34:** 675–679.

29. Wang, X. H., H. Ushio, and T. Ohshima. 2003. Distributions of hydroperoxide positional isomers generated by oxidation of 1-palmitoyl-2-arachidonoyl-*sn*-glycero-3-phosphocholine in liposomes and in methanol solution. *Lipids.* **38:** 65–72.
30. Miyazawa, T., and T. Hayashi. 1998. Age-associated oxidative damage in microsomal and plasma membrane lipids of rat hepatocytes. *Mech. Ageing Dev.* **100:** 231–242.
31. Kinoshita, M., S. Oikawa, K. Ayasaka, A. Sekikawa, T. Nagashima, T. Toyota, and T. Miyazawa. 2000. Age-related increases in plasma phosphatidylcholine hydroperoxide concentrations in control subjects and patients with hyperlipidemia. *Clin. Chem.* **46:** 822–828.
32. Moriya, K., K. Nakagawa, T. Santa, Y. Shintani, H. Fujie, H. Miyoshi, T. Tsutsumi, T. Miyazawa, K. Ishibashi, T. Horie, et al. 2001. Oxidative stress in the absence of inflammation in a mouse model for hepatitis C virus-associated hepatocarcinogenesis. *Cancer Res.* **61:** 4365–4370.
33. Nagashima, T., S. Oikawa, Y. Hirayama, Y. Tokita, A. Sekikawa, Y. Ishigaki, R. Yamada, and T. Miyazawa. 2002. Increase of serum phosphatidylcholine hydroperoxide dependent on glycemic control in type 2 diabetic patients. *Diabetes Res. Clin. Pract.* **56:** 19–25.
34. Tokita, Y., Y. Hirayama, A. Sekikawa, H. Kotake, T. Toyota, T. Miyazawa, T. Sawai, and S. Oikawa. 2005. Fructose ingestion enhances atherosclerosis and deposition of advanced glycated end-products in cholesterol-fed rabbits. *J. Atheroscler. Thromb.* **12:** 260–267.